Midkine and Pleiotrophin in *Drosophila*

by

Jeff Chen

A Dissertation

Presented to the Department of Cell and Developmental Biology

and the Oregon Health & Sciences University School of Medicine

in partial fulfillment of

the requirement for the degree of

Doctor of Philosophy

December 2007

School of Medicine
Oregon Health & Science University

CERTIFICATE OF APPROVAL

This is to certify that the Ph.D. thesis of

Jeff Chen

has been approved

Mentor/Advisor

Member

Member

Member

Table of Contents

Acknowledgements

I am grateful for the advice of Dr. Joseph Weiss, my thesis mentor. I would like also to thank my thesis committee members Dr. Doris Kretzschmar, Dr. Mike Liskay, and Dr. Ronen Schweitzer for their guidance and support.

I am indebted to Dr. Philip Copenhaver, Dr. Mike Forte, Dr. Karla Kent, Dr. David Morton and Dr. Sarah Smolik for giving invaluable input on my project. I also want to express my gratitude to the members of the Weiss, Kretzschmar, and Morton labs, and in particular Dr. Dennis Hazelett, Dr. Priya Mani, and Jill Wentzel for their constant support over the years. I also want to thank Jacqueline Parker, who taught me valuable laboratory techniques in working with *Drosophila.* I am also deeply appreciative for the intellectual support of Dr. Daniel Pankratz, who has given me countless advices as I progressed towards the finish line.

I wish to express my gratitude for the support and encouragement of Dr. James Lundblad, who was responsible for bringing me to OHSU and has taken a personal interest in my success. I would also like to thank Dr. Peter Sullivan, a great teacher who has taught me valuable clinical skills and who has kept them sharp over the graduate school years.

I also want to thank Erin and Nick Statkus, Jenna and Josh Hill, who have "adopted" me over the years as I have been away from my family. Erin, Nick, Jenna, Josh, thank you for being family and keeping my spirits up over the years.

And finally, thank you Mom and Dad. I finally did it. None of this would have been possible without your love, sacrifice, dedication, and support from the very

beginning. Thank you for believing in me and giving me the opportunity to strive for success.

Abstract

Midkine and Pleiotrophin are heparin-binding, secreted small molecules that elicit a variety of process in tissue culture, including neurite outgrowth, branching morphogenesis, chemotaxis, angiogenesis, cell proliferation and survival. Biochemical chemical binding assays have identified a number of molecules that may function as receptors. In this thesis work I investigated the biological functions of Midkine and Pleiotrophin by characterizing the *Drosophila* homologues Miple1 and Miple2. My expression data suggested that *miple1* is expressed in central nervous system (CNS) glia during embryogenesis, in proliferating cells in the CNS in larvae, and in the mushroom body in the adult brain. *miple2* is expressed in the embryonic endoderm and mesoderm, the larval imaginal discs, and the adult gonads. I used a *miple2*-null mutant to investigate the requirement for Miple2 in Anaplastic lymphoma kinase (Alk) signaling, and in the Wingless/Wnt, Hedgehog, Decapentaplegic (Dpp)/TGFβ signaling pathways. Combined developmental and genetic data do not support Miple2 as a component in Alk signaling. My results are inconclusive in determining the requirement for Miple2 in Wingless, Hedgehog, and Dpp/TGFβ signaling. I also report a potential male sterile phenotype caused by defective sperm individualization in the *miple2*-null mutants.

Chapter 1

Introduction

Introduction

Cells in a multicellular organism communicate via cell-cell signaling, which mediates important biological activities, such as cell proliferation, differentiation, and cell death. The coordination of these cellular events is central to development and disease. A common form of cell-cell communication involves a secreted signaling molecule which, via a cell surface receptor and downstream components of the signaling pathway, elicits a variety of responses in the target cell. The goal of the work presented here was to determine the role of two secreted molecules with proposed function in signaling, Midkine and Pleiotrophin, that are ubiquitously expressed during embryonic development. In adults, however, elevated expression levels are associated with pathological conditions[1].

Midkine and Pleiotrophin are two closely related, low molecular weight, secreted molecules that bind heparin and heparan sulfate (HS). HS are glycosaminoglycans (GAGs), which are long, unbranched polysaccharides made up of repeating disaccharide units. They constitute a significant component of the extracellular matrix (ECM). Midkine and Pleiotrophin, therefore, are likely to mediate their signaling functions by interacting with HS on the cell surface. HS is attached to proteins found on the cell surface and the ECM, and it binds to a variety of secreted ligands.

Tissue culture experiments suggest that Midkine and Pleiotrophin promote neurite outgrowth, cell migration, branching morphogenesis, cell proliferation, and cell survival. Biochemical approaches have identified a number of molecules that bind Midkine and Pleiotrophin and may function as receptors *in vivo*. Loss-of-function mutant mice

deficient in both molecules do not provide mechanistic data for understanding Midkine and Pleiotrophin function *in vivo*.

Midkine was initially identified as a retinoic-acid inducible gene product in cell lines derived from the mouse embryonic carcinoma[2, 3]. It has a molecular weight of 13 kD. Amino acid sequence analysis shows that it bears a high degree of homology to Pleiotrophin, an 18-kD molecule initially identified as a neurotrophic factor from the rat brain and as a bovine uterus-derived fibroblast mitogen by two independent groups[4, 5]. Chicken Midkine is also known as retinoic acid-induced binding factor, or RIHB[3]. Alternative names for Pleiotrophin include heparin binding growth-associated molecule, (HB-GAM), OSF-1, heparin associated regulatory protein (HARP), and heparin binding neurotrophic factor (HBNF) [6-8]. Together, Midkine and Pleiotrophin are the only members of the protein family. They are conserved across the metazoan kingdom.

Tissue culture and gain-of-function studies

Neurite outgrowth

Since Pleiotrophin is initially isolated from the brain, and Midkine is the only other homologue in the vertebrate genome, both molecules have been proposed to have neurotrophic functions. *In vitro* experiments with primary tissue culture cells of the nervous system demonstrated that both Midkine and Pleiotrophin are capable of promoting neurite outgrowth. Neonatal rat cortical neurons extend neurites that form networks and fasciculate when grown on Midkine-coated tissue plates[9]. Pleiotrophin has also been reported to promote neurite outgrowth from embryonic neurons in tissue culture[10].

Since "neurite" is a collective term referring to any projection extending from a neuronal cell body, the outgrowths observed *in vitro* could represent either axon or dendrite. Therefore, Midkine and Pleiotrophin could function as factors in either axon guidance or synapse formation, or both. However, as the current knowledge base on Midkine and Pleiotrophin as neurotrophic factors lack functional *in vivo* data from loss-of-function mutants, their precise roles in the nervous system remain to be determined.

Cell migration

Neurite outgrowth involves changes in cell shape, a process observed in additional biological processes, including cell migration. Tissue culture experiments suggest that both Midkine and Pleiotrophin are capable of inducing migration of rat embryonic cortical neurons [11, 12]. Both molecules may function as chemoattractants for additional cell types. Bone marrow progenitor cells migrate toward Midkine and Pleiotrophin in tissue culture, and Midkine-dependent osteoblast migration requires the activation of both phosphatidylinositol kinase (PI3K) and mitogen activated protein kinase (MAPK) signaling pathways[13, 14]. Midkine-induced neutrophil migration requires G-protein coupled receptor signaling, as well as the PI3 and MAP kinase signaling pathways[15]. Although published data suggests that Midkine and Pleiotrophin may function as chemoattractants, the absolute requirement for these molecules to induce cell migration *in vivo* cannot be established. While the ubiquitous expression patterns of Midkine and Pleiotrophin *in vivo* suggest that they may function as permissive signals for cell migration, existing data do not exclude the possibility that they could act as instructive cues that guide cell migration.

Branching morphogenesis

Cell shape change is also observed in cells undergoing branching morphogenesis, which refers to the formation of branched epithelial tubules during development. Midkine and, to a lesser degree, Pleiotrophin, are expressed in the embryonic kidney and lung, where epithelially derived tissues form the collecting tubules and the bronchial tree, respectively[16]. In tissue culture, the addition of Midkine or Pleiotrophin purified from conditioned kidney mesenchyme media induced branching morphogenesis of embryonic rat ureteric bud explants[17, 18]. A similar observation is made in the developing lung tissue, as the addition of Midkine induced a weak effect on the branching morphogenesis of mouse embryonic lung explants[19]. While the *in vitro* experiments indicate that both molecules are sufficient to induce branching morphogenesis, their requirement in the process remains to be determined *in vivo*.

Anti-apoptosis/Cell survival

Investigations into the neurotrophic effects of Midkine and Pleiotrophin revealed that they protect cells against apoptosis, or programmed cell death, *in vitro*. Addition of Midkine to the media protects serum-starved primary mouse cortical neurons against apoptosis by inhibiting the activation of caspase-3, a protease required for the initiation of the apoptotic process. The protective effect is correlated with the phosphorylation of both the MAP kinase and Akt, components of the MAP kinase and PI3 kinase signaling pathways, respectively[20]. Similar observations have also been reported when Midkine is added to culture medium of human hepatocellular carcinoma cells and human meningioma cells[21, 22]. *In vivo* gain-of-function experiments are consistent with

observation in tissue culture. In peri-infarct areas in the post-ischemic injury mouse brain, decreased TUNEL-positive apoptotic cells and decreased activated caspase-3 immunoreactivity are correlated with the expression of Midkine from an adenovirus vector[23].

Additional published results implicate Bcl-2, an anti-apoptotic protein, as a potential downstream component of Midkine-mediated cell survival. *In vivo* mouse model suggests that cisplatin-induced apoptosis in renal tubular cells is correlated with decreased Midkine expression. Tissue culture experiments using Wilm's tumor cell lines demonstrated that exogenous Midkine reduced cisplatin-induced apoptosis in a dose-dependent manner, and the protective effect is correlated with increased expression of the anti-apoptotic Bcl-2[24].

Pleiotrophin's effects on apoptosis have also been investigated. *In vitro* studies have demonstrated that Pleiotrophin protects both epithelial derived SW-13 cells and NIH3T3 fibroblasts against apoptosis via the PI3 kinase signaling pathway[25, 26].

While the aforementioned studies suggest that Midkine and Pleiotrophin may protect against apoptosis, the data is limited to gain-of-function studies in which Midkine and Pleiotrophin are exogenously supplied to cells in tissue culture. They do not unequivocally demonstrate that promoting cell survival is a biological function of Midkine and Pleiotrophin.

Mitogenicity

Multiple groups have published results suggesting that Midkine has mitogenic properties *in vitro*. When added to tissue culture medium, recombinant mouse Midkine

increased thymidine uptake in NIH3T3 mouse fibroblast cells[9]. Tissue culture studies on cells derived from rhabdoid tumor of the kidney demonstrated that Midkine-dependent cell proliferation is correlated with tyrosine phosphorylation of the components of the Jak/Stat signaling pathway[27]. Moreover, stimulation of human adrenal tumor derived SW13 cells with Midkine increased their anchorage-independent colony formation in soft agar, and these cells demonstrate increased tumorgenicity when transplanted into athymic nude mice [28]. On the other hand, treatment of mouse rectal carcinoma cells, which normally express Midkine, with antisense oligodeoxynucleotide against Midkine reduced these cells' ability to form colonies in soft agar and their tumorgenicity when transplanted into nude mice[29]. Taken together, these data suggest that Midkine may be sufficient to induce cell proliferation. However, neither tissue culture nor *in vivo* data provide convincing evidence that the increased cell proliferation is the direct effect of Midkine.

Pleiotrophin's ability to promote cell proliferation in tissue culture has also been reported. However, published data from organ culture and *in vivo* observations contradict *in vitro* findings. Both bovine uterus-derived and recombinant human Pleiotrophin are capable of promoting NIH3T3 fibroblast cell proliferation[4, 10]. Like Midkine, Pleiotrophin also promotes the anchorage-independent colony formation in human adrenal tumor derived cells[30]. Tissue culture experiments using epithelial cells from bovine eye lens suggest that cell proliferation in the presence of Pleiotrophin is correlated with the activation of MAP kinase and PI3 kinase signaling pathways[31].

While fibroblast and primary culture cells increase proliferation in response to Pleiotrophin, the addition of Pleiotrophin to explanted developing rat limb buds in tissue

culture inhibits cell proliferation, as measured by decreased BrdU uptake. Consistent with such a finding, both Pleiotrophin mRNA and protein expression colocalize with quiescent cells in the developing rat limb bud *in vivo*[32]. The same group reported that the developing cerebral cortex of mouse deficient in the Pleiotrophin gene demonstrated increased BrdU uptake, and the mature cortex in these mice have increased cellularity compared to littermates heterozyogous for the pleiotrophin gene[33]. The inconsistencies between Pleiotrophin's *in vitro* and *in vivo* effect on cell proliferation, and the lack of descriptions of a clear phenotype in Midkine-deficient mice, cast doubt on the theory that Midkine and Pleiotrophin function as bona fide mitogens in the biological context.

Angiogenesis

Pleiotrophin and, to a lesser degree, Midkine, have been reported to have angiogenic properties in both *in vitro* and *in vivo* studies. Recombinant human Pleiotrophin is mitogenic towards endothelial cells and is capable of inducing angiogenesis *in vitro*[34]. In the rat brain following ischemic injury, Pleiotrophin mRNA expression and immunoreactivity colocalize with endothelial cell markers in the peri-infarct areas[35]. When transplanted into athymic nude mice, transformed breast carcinoma cells stably expressing either Pleiotrophin or Midkine form tumors with higher levels of vascularization compared to tumors that arose from untransformed control cells. In the same study, transplantation of either Midkine- or Pleiotrophin-expressing cells into the normally avascular rabbit cornea induced neovascularization compared to the control[36]. More recently, one group reported that the introduction of Pleiotrophin-expressing plasmid into the post-ischemic injury rat myocardium induces the formation of normal

appearing capillaries and arterioles that interconnect with the existing coronary vascular system[37]. Attempts have been made to elucidate the mechanism of Pleiotrophin's angiogenic properties. Using specific pharmacologic inhibitors of signaling, one group presented data suggesting that Pleiotrophin promotes angiogenesis on human umbilical vein endothelial cells (HUVECs) *in vitro* via the activation of the inositol-3-phosphate kinase (PI3K) signaling pathway[38].

While most published data suggest that Midkine and Pleiotrophin promote angiogenesis, one recent study, reported that Pleiotrophin inhibits vascular endothelial growth factor- (VEGF) dependent endothelial cell proliferation and tubular formation *in vitro* by binding to the VEGF and inhibiting its binding to the receptor[39]. Taken together, these findings illustrate the complexity of the roles of Midkine and Pleiotrophin in regulating angiogenesis. More importantly, since these findings are based on gain-of-function studies derived from systems overexpressing Mikine and Pleiotropin, they do not unambiguously establish angiogenesis as a biological function of these molecules.

Putative receptors of Midkine and Pleiotrophin

Since Midkine and Pleiotrophin are secreted molecules that elicit a wide range of cellular responses when added to cells in culture, they have been proposed to be signaling molecules. Various groups, relying on *in vitro* binding assays, have identified a number of structurally unrelated molecules that biochemically interact with Midkine and Pleiotrophin.

Both Midkine and Pleiotrophin have been reported to bind Anaplastic lymphoma kinase (ALK), a receptor tyrosine kinase (RTK) [40]. In the inactive state, RTK exists in the

unphosphorylated mononeric form. Upon the binding of an activating ligand, the receptor dimerizes, and the intracellular tyrosine kinase domains cross phosphorylate, recruit the binding of docking molecules that lead to the formation of an active signaling complex which, via the activation of the downstream mitogen activated protein kinase (MAPK) or phosphatidylinositol-3 kinase (PI3K) pathways, exerts a variety of cellular responses[41].

ALK was initially identified as a human proto-oncogene[42, 43]. It was identified as a binding partner to Pleiotrophin from a panned phage display of a human cDNA library using immobilized Pleiotrophin protein as bait[25]. Proposed binding of Pleiotrophin to ALK activates both the MAP kinase and PI3 kinase signaling pathways in SW-13; both pathways are required in Pleiotrophin-dependent cell proliferation, but only the MAP kinase signaling pathway is required in promoting cell survival[26]. The same group also published findings that Midkine bind to ALK, but with a six-fold lower affinity than that of Pleiotrophin. As in the case of Pleiotrophin, addition of Midkine to ALK-expressing human SW-13 cells activated the MAP kinase and PI3 kinase signaling pathways and led to increased anchor-independent cell proliferation in soft agar and protection against apoptosis[28, 44]. Expression data in mice and rats lend support to the contention that ALK may be a biological receptor for both Midkine and Pleiotrophin. *In situ* hybridization demonstrates that *alk* mRNA expression in mice overlaps spatially and temporally with Midkine and Pleiotrophin mRNA expression during embryogenesis and in adulthood[40, 45].

Protein tyrosine phosphatase ζ (PTPζ), alternatively known as receptor protein tyrosine phosphatase β (RPTPβ), also binds both Midkine and Pleiotrophin *in vitro*[46, 47]. RPTPβ/ PTPζ belongs to a family of molecules known as receptor protein tyrosine phosphatases (RPTPs), which are type I transmembrane proteins with an intracellular

catalytic domain that has phosphatase activity. Together with protein tyrosine kinases, RPTPs regulate the phosphorylation state of intracellular components of receptor tyrosine kinase (RTK) signaling pathways. Most RPTPs are orphan receptors with no known biological ligands, and the mechanism of RPTP action is poorly understood. RPTPs form homophilic interactions, and dimerization has been proposed to inactivate the phosphatase activity of CD45, an immune system-specific RPTP[48, 49]. Crystal structure analysis of RPTPα suggests that dimerization blocks substrate access to the intracellular phosphatase domain[50]. An alternative model suggests that dimerization causes *trans*-dephosphrylation of positively activating phosphotyrosine residues within the catalytic domain[51].

Pleiotrophin from rat brain extract microsomal fractions was found to bind to purified 6B4 proteoglycan, the extracellular component of PTPζ, in affinity chromatography[52]. Tissue culture experiment findings suggest that PTPζ is required for Pleiotrophin-dependent neurite outgrowth and neuronal migration[12, 52]. Pleiotrophin is most likely an inhibitory ligand and exerts mitogenic, neurite outgrowth, anti-apoptotic, and chemotactic effects by inhibiting PTPζ-dependent dephosphorylation of β-catenin, Fyn, and β-adductin[53-55].

Solid phase binding assays also demonstrate that Midkine is also capable of binding RPTPβ/PTPζ[11]. Tissue culture findings suggest that RPTPβ/PTPζ mediates Midkine-dependent cell migration and neuronal survival[14, 56]. RPTPβ/PTPζ is expressed in both the embryonic and adult brain, and the pattern of expression overlaps with those of Midkine and Pleiotrophin[57]. While these *in vitro* data are based purely on biochemical interactions, behavioral analyses on RPTPβ/PTPζ loss-of-function mice revealed

maturation-dependent learning deficits reminiscent of those seen in Midkine- and Pleiotrophin-null mice[58-60].

While the potential interactions between Midkine or Pleiotrophin, and PTPζ as the ligand-receptor pair in signaling have been extensively documented, additional proteins have been identified as receptors for Midkine and Pleiotrophin based on *in vitro* binding assays, and new ones are likely to emerge. One class of molecules that bind Midkine and Pleiotrophin are heparan sulfate proteoglycans (HSPGs), which consist of a core protein to which one or more glycosaminoglycan chains are attached to the specific sites. They have been proposed to function as cofactors in signaling. Midkine binds to Syndecan-1, Syndecan-3 (N-syndecan), and Syndecan-4 (Ryoducan), all of which are heparan sulfate proteoglycans with a single transmembrane domain and are thought to function as cofactors in signaling[61, 62]. Pleiotrophin, on the other hand, binds exclusively to Syndecan-3[63]. Tissue culture experiments indicate that binding of Midkine or Pleiotrophin to Syndecans are capable of promoting neurite outgrowth *in vitro*. In addition, Midkine binds Glypican-2, a heparan sulfate proteoglycan anchored to the cell surface via a glycosylphosphatidylinositol (GPI) anchor, and the binding also caused neurite outgrowth in tissue culture[64].

Binding assays have also identified Neuroglycan-C, a chondroitin sulfate proteoglycan, as a potential receptor for Midkine-dependent oligodendrite process outgrowth[65]. Versican, a chondroitin sulfate proteoglycan with proposed functions in cell migration and proliferation, also binds Midkine *in vitro*[66]. In addition to proteoglycans, LRP-1, an LDL-receptor related protein, binds Midkine *in vitro*[67]. LRP-1 binding of

Midkine has been suggested to mediate the internalization and nuclear localization of Midkine, a process proposed to be required for Midkine dependent cell survival[68].

It must be noted that the growing list of proteins that bind Midkine and Pleiotrophin have been identified based on biochemical binding assays. Despite their diverse structure and biochemical function, published data are not mutually exclusive. However, whether these molecules function as biological receptors *in vivo* remain to be determined, and a potentially clarifying approach involves phenotypic comparisons between the loss-of-function mutants in Midkine, Pleiotrophin, and their putative receptors in a model organism.

Midkine and Pleiotrophin structure

The structure of Midkine and Pleiotrophin in solution has been solved by NMR[69, 70]. Both molecules have two homologous domains, named N-domain and C-domain, respectively. Each domain is characterized by three anti-parallel beta sheets and basic amino acid residues that form positively charged clusters on the surface. Space filling models of Midkine suggest that the basic amino acids are required for binding heparin, and the binding of heparin converts Midkine into the active dimer form[69]. The N- and C-domains belong to a motif known as the Thrombospondin structural homology repeat, or TSR, which are typically found in proteins that mediate cell-to-extracellular matrix and cell-to-cell adhesions[70, 71]. Cysteine residues within each domain form intra-domain disulfide bridges[72, 73]. The two TSR motifs are linked together random coils that do not exhibit homology to any known motifs.

The potential activity of each domain has been mapped using recombinant Midkine and Pleiotrophin. The C-terminal domain of both proteins is capable of promoting neurite outgrowth in tissue culture[74, 75]. Site-directed mutagenesis against the basic amino acid residues within the C-domain of Midkine abolished its neurite outgrowth activity, suggesting that these residues are functionally significant[76]. In addition, tumors arising from SW-13 cells transformed with the truncated Pleiotrophin consisting of only the C-domain led to vascularization in nude mice, suggesting that the C-domain is sufficient for angiogenesis[77]. Truncated Midkine consisting of only the C-domain, however, is not sufficient to protect primary culture neurons against apoptosis[74].

While the C-domain of either Midkine or Pleiotrophin is sufficient to recapitulate most of the published *in vitro* activity elicited by the intact protein, truncated Midkine or Pleiotrophin lacking it is largely inactive. The N-domain of Pleiotrophin is capable of inducing NIH3T3 fibroblasts to undergo anchorage-independent colony formation in soft agar, thereby suggesting that the N-domain is alone is sufficient for transformation[77]. When the nonconserved region between the two domains in Pleiotrophin is replaced by glycine, the neurite outgrowth activity is retained, suggesting that the linker region may not be required for activity[78].

Structural homologues of Midkine and Pleiotrophin are conserved across the metazoan kingdom, from *Drosophila* to humans. The retention of the Midkine and Pleiotrophin, and the C-domain in particular, throughout 400 million years of evolution suggests that these molecules play significant biological roles, which to this day remains to be determined in the physiological context.

Midkine and Pleiotrophin expression *in vivo*

Current knowledge on the expression patterns of Midkine and Pleiotrophin primarily derive from studies in mice and rats. During embryogenesis, Midkine and Pleiotrophin are expressed in the central and peripheral nervous systems and at sites where epithelial-mesenchymal interactions take place [2, 16]. Midkine levels peak during midgestation period and decreases perinatally, while Pleiotrophin is expressed highly around the time of birth and maintained at low levels in neural tissues.

Midkine and Pleiotrophin expression during neurogenesis have been well described. The expression patterns of both proteins correlate temporally with cell proliferation and axon pathfinding in the developing central nervous sytem. In both mouse and rat embryos, high levels of Pleiotrophin mRNA localizes to the periventricular region of the embryonic brain and the neuroepithelium lining the central canal of the developing spinal cord, where neuronal precursors undergo mitosis. Midkine and Pleitrophin proteins are localized to neuronal and glial processes along the axon tracts, and these findings are consistent with their extracellular nature[16, 79, 80]. Midkine expression in the central nervous system decreases significantly prior to birth, while that of Pleiotrophin persists postnatally. In adult mice, Pleiotrophin mRNA is expressed in the hippocampus and the Purkinje cells of the cerebellar cortex, while the Pleiotrophin protein localizes to the axon tracts of the hippocampal and Purkinje neurons[81, 82]. While it is noteworthy that the synapses in both locations demonstrate activity-dependent synaptic plasticity, the role of Pleiotrophin in synaptic restructuring cannot be directly established.

Outside of the nervous sytem during embryogenesis, both Midkine and Pleiotrophin are primarily expressed where epithelial-mesenchymal interactions take

place. These locations include the kidneys, lungs, and teeth. In both the kidneys and the lungs, Midkine is the predominant protein, and it is found primarily in the epithelially-derived collecting tubules and the tracheal tree[16, 17, 83]. Pleiotrophin is expressed in a similar pattern[16].

The expression patterns of Midkine and Pleiotrophin during development provide correlative data suggesting that both proteins may possess functions revealed in tissue culture studies. That Midkine and Pleiotrophin are found in the nervous system suggest that they have neurotrophic functions. On the other hand, the presence of Midkine and Pleiotrophin in the developing kidneys and lungs lend support to the tissue culture finding that they promote branching morphogenesis. These functions, however, remain to be determined by analysis of loss-of-function mutants *in vivo*.

Midkine and Pleiotrophin in disease

While Midkine and Pleitrophin are ubiquitously expressed during embryogenesis, high levels of expression in adulthood are correlated with pathological conditions. Midkine expression is associated with neoplastic diseases. Over 80% of carcinomas of the gastrointestinal tract overexpress Midkine. In prostate carcinoma, Midkine is detectable at a very early stage. Midkine expression is the hallmark of Wilm's tumor, which involves the deletion of the tumor suppressor gene WT-1. WT-1 binds to the promoter region of MK gene and acts as a transcriptional repressor. The loss of WT-1 leads to Midkine overexpression, which has been proposed to act in an autocrine manner in promoting tumor growth. Strong expression of Midkine is a poor prognostic marker for neuroblastoma, glioblastoma, and urinary bladder carcinoma. Pleiotrophin expression, on

the other hand, is relatively restricted in tumors. Since tumor overexpression leads to elevated serum proteins, Midkine and Pleiotrophin may be used as diagnostic markers[1].

Midkine and Pleiotrophin expression are also correlated with neurodegenerative diseases. Senile plaques from Alzheimer's disease patients are immunoreactive with both Midkine and Pleiotrophin[84, 85]. In addition, Alzheimer's patients have elevated Midkine levels in serum[86]. Midkine protein is also found in Down's syndrome placques and neurofibrillary plaques from patients with Lytico-Bodig disease[85, 87].

Chronic inflammatory states are also correlated with Midkine or Pleiotrophin expression. Both RT-PCR and ELISA results indicate the presence of Pleiotrophin in the synovial fluid of rheumatoid arthritis patients[88]. Midkine is present in the synovial fluids of patients suffering both both degenerative and rheumatoid arthritis[89]. However, animal model experiments suggest that Midkine and Pleiotrophin expression in inflammatory states may be a part of the tissue repair process. Midkine immunoreactivity is found in fibroblasts in tissues surrounding lesions in gastric ulcers and chronic colitis in rats[90, 91]. In mice, fibroblasts surrounding cutaneous wounds express Pleiotrophin[92].

Post-ischemic tissues are immunoreactive with both Midkine and Pleiotrophin, suggesting that both proteins may be involved in the repair process. Following cerebral ischemia in rat models, astrocytes, macrophages, and endothelial cells express both Midkine and Pleiotrophin in the peri-infarct areas[35, 93, 94]. *In vivo* data suggest that Midkine is also found in the peri-infarct areas in myocardial infarcts[95]. Analysis of Midkine-null mice revealed a potential protective effect of Midkine in post-ischemic injury, as the infarct volume and the number of myocardiocytes undergoing apoptosis is reduced in wild type mice[96].

Mouse mutants in Midkine and Pleiotrophin

Current understandings of Midkine and Pleiotrophin function derive primarily from *in vitro* gain-of-function studies. They shed little light on the true biological functions of these molecules *in vivo*. Observations of Midkine and Pleiotrophin *in vivo* during both development and disease provide correlative data that do not establish a causal relationship between gene expression and physiological function. The most definitive approach to elucidating the biological functions of Midkine and Pleiotrophin involves the phenotypic analysis of loss-of-function mutants in model genetic systems. Toward this end mice deficient in either Midkine or Pleiotrophin have been generated. Both Midkine- and Pleiotrophin-null mice are viable and fertile, and phenotypic analyses of organs that express Midkine or Pleiotrophin reveal no gross structural defects[59, 81]. More detailed analysis of Pleiotrophin-null mice revealed increased neuronal number in the adult cerebral cortex secondary to enhanced proliferation of ventricular zone neural stem cells in the embryo[33]. Behavioral studies revealed that both Midkine-null and Pleiotrophin-null mice exhibit increased anxiety and deficits in memory, which resolved in Midkine-null mice six weeks after birth[59, 60]. On the other hand, mice overexpressing Pleiotrophin display behavioral phenotype opposite that of the Pleiotrophin-null mutants, suggesting that the behavioral phenotype is specific to the loss of Pleiotrophin[60]. Despite these findings, available genetic data do not provide any insight into mechanisms that link Midkine or Pleiotrophin to observed behavioral phenotype.

The absence of a gross structural phenotype in Midkine- or Pleiotrophin-null single mutants suggests a possible functional redundancy between the two molecules, given their structural similarity and overlapping patterns of expression during

development. Analysis of Midkine-null mouse revealed increased levels of Pleiotrophin mRNA and protein expression; on the other hand, loss of Pleiotrophin does not affect Midkine expression[97]. In order to address the functional redundancy of Midkine and Pleiotrophin *in vivo*, a loss-of-function *Mk-/-; Ptn-/-* double mutant mouse has been generated. The double mutants are born in only one third the Mendelian ratio, exhibit hearing deficits secondary to the loss of expression of β-tectorin, which encodes the major non-collagen protein in the cochlea and is required for sound conductance[98]. Most, but not all, of the female double mutants are sterile. They have reduced number of mature follicles and ova, exhibit longer diestrus and proesterus periods and shorter estrus periods; moreover, half of the double mutant females have vaginal abnormality[99].

The report of the *Mk-/-; Ptn-/-* double mutant mouse phenotype suggests a requirement of these genes in auditory system and the female reproductive cycle. However, a number of issues remain unresolved. That the double mutants are born at only one third the expected Mendelian ratio suggests the issue of penetrance. It is entirely possible that the loss of both Midkine and Pleiotrophin disrupts the development of organs where the two genes are expressed during embryogenesis and lead to an unreported early embryonic lethal phenotype. The biological mechanisms underlying auditory system and the female reproductive tract development is complex and poorly characterized. Consequently, a direct link between Midkine and Pleiotrophin and the double mutant phenotypes is complex and difficult to establish. A different model organism, therefore, may provide better understanding on Pleiotrophin and Midkine function *in vivo*.

Conservation of Midkine and Pleiotrophin in *Drosophila*

Midkine and Pleiotrophin are conserved across the metazoan kingdom, from humans to invertebrates[1]. In *Drosophila* melanogaster, the homologues are known as Miple1 and Miple2 (Midkine and Pleiotrophin), respectively. Both proteins are secreted molecules. During the course of my study, protein sequence analysis reported by another group revealed the conservation of the functional domains and key amino acids between Midkine, Pleiotrophin, Miple1, and Miple2[100].

The conservation of Midkine and Pleiotrophin in *Drosophila* makes it a logical *in vivo* model system for understanding Midkine and Pleiotrophin biological function. More than two thirds of the known human disease genes have homologues in *Drosophila*. In addition, the same signaling pathways in mammalian development are conserved in *Drosophila*. Indeed, all of the putative receptor molecules for Midkine and Pleiotrophin have homologues in *Drosophila*. Genetic studies over the last century have established *Drosophila* as an ideal system for genetic manipulation. *Drosophila* has a compact genome, with four chromosomes encoding 15,000 genes. Consequently, analysis of *Drosophila* mutant phenotypes poses a lesser challenge due to fewer genetic redundancies. Furthermore, genome wide mutagenesis intended to disrupt every single gene in *Drosophila* is underway, and products of these mass mutagenesis efforts are available to the research community. The most significant factor making *Drosophila* the most ideal system for investigating the biological functions of Midkine and Pleiotrophin is the power of phenotypic analysis. Over the past several decades many signaling pathways and biological processes have been thoroughly characterized with respect to their roles in *Drosophila* development. Mutations observed in *Drosophila* can be rapidly

assigned to a signaling pathway based on its phenotype. The combination of conserved biological processes, amenity to genetic manipulation, and phenotypic correlation makes *Drosophila* an ideal *in vivo* system to uncover Midkine and Pleiotrophin function.

Chapter 2

miple1 and *miple2* expression during *Drosophila* development

Abstract

Midkine and Pleiotrophin are heparin-binding, secreted small molecules with proposed functions in signaling. In tissue culture, they promote cell proliferation, cell survival, neurite outgrowth, branching morphogenesis, and migration. The homologues in *Drosophila* are Miple1 and Miple2. In this chapter, I characterized the expression patterns of *miple1* and *miple2* genes throughout *Drosophila* development. *miple1* is expressed by the glial cells in the central nervous system throughout *Drosophila* development. Embryonic *miple2* expression localizes to the endoderm and the mesoderm. During post embryonic development, *miple2* is primarily expressed in the larval imaginal discs and gonads in both adult males and females. The data presented in this study provides the basis for future investigations using phenotypic correlation in *Drosophila* development to understand the biological functions of Midkine and Pleiotrophin.

Introduction

Midkine and Pleiotrophin make up a family of secreted heparin-binding small molecules with proposed functions in signaling. Tissue culture experiment results have demonstrated that they promote neurite outgrowth, cell migration, branching morphogenesis, angiogenesis, cell proliferation and cell survival[9-12, 17, 18, 20, 25, 36]. Biochemical binding assays have identified a number of structurally unrelated transmemebrane molecules with distinct biochemical functions as putative receptors for Midkine and Pleiotrophin. Elevated Midkine and Pleiotrophin serum levels in adult humans are correlated with disease conditions[101]. Studies in mice have demonstrated that both proteins are expressed in overlapping patterns during embryogenesis[16]. To date, attempts to identify the biological functions of Midkine and Pleiotrophin function using loss-of-function mutants in mice have not been informative. Single mutant mice exhibit no gross structural defects[59, 81]. Although *mk-/-; ptn-/-* double mutant mice have auditory defects and are female sterile, phenotypic analyses have not revealed molecular mechanisms underlying Midkine and Pleiotrophin function[98, 99].

Midkine and Pleiotrophin are conserved across the metazoan kingdom, from humans to invertebrates[1]. In *Drosophila* melanogaster, there are two homologues, known as Miple1 and Miple2, (Midkine and Pleiotrophin), respectively. Amino acid sequence alignment between human Midkine and Pleiotrophin and *Drosophila* Miple1 and Miple2 revealed a high degree of conservation: the overall amino acid sequence similarity with human Midkine is 66% for Miple1 and 58% for Miple2; homology with human Pleiotrophin is 60% for Miple1 and 58% for Miple2. The key amino acid residues and structural motifs are conserved between Miple1, Miple1, and Midkine and Pleiotrophin.

Detailed sequence analysis reveals that both Miple1 and Miple2 contain secretory signals. This prediction is confirmed by the finding that both proteins are found in the conditioned medium when expressed in tissue culture cells[100].

The signaling pathways in development are highly conserved between mammals and *Drosophila*. In addition, all of the transmembrane molecules identified as binding partners for Midkine and Pleiotrophin in biochemical experiments have homologues in *Drosophila*. The compactness of the *Drosophila* genome, which consists of only four chromosomes encoding 15,000 genes, presents less challenge arising from genetic redundancy, which may complicate mutant phenotype analysis[102]. Moreover, the *Drosophila* genome has been the subject of large scale saturation mutagenesis, and the products of the mutagenesis efforts are available to the entire *Drosophila* research community[103-105].

The combination of the high degree of conservation between the signaling pathways and the biological processes between humans and fruit flies, the simplicity of the *Drosophila* genome, as well as its amenability to genetic manipulation, makes *Drosophila* an attractive model organism for elucidating Midkine and Pleiotrophin function. Tissues from different stages of *Drosophila* development have been established as *in vivo* model systems for dissecting the signaling pathways. The embryonic central nervous system and the larval optic lobe have been used to uncover the molecular mechanism underlying axon guidance. Combined developmental and genetic data from analyses of embryos defective in mesoderm, tracheal system, and germ cell development have provided insight into signaling mechanisms regulating cell migration and branching morphogenesis. The larval wing imaginal disc, consisting of epithelial tissues that

undergo extensive proliferation and remodeling under the control of developmentally conserved signaling pathways, serves as a model system for understanding morphogen signaling.

To date, only the mRNA expression patterns of *miple1* and *miple2* during embryogenesis have been characterized. The onset of *miple1* expression occurs during mid embryogenesis, and *miple1* mRNA primarily localizes to the central nervous system throughout the embryogenesis. On the other hand, *miple2* is expressed during early embryogenesis in the mesoderm and the endoderm[100]. Expression patterns of both genes during post embryonic stages of development remain to be determined. In this study, I seek to expand the characterization of *miple1* and *miple2* expression during embryogenesis. I will also analyze Miple1 protein distribution using rabbit anti-Miple1 antiserum. In addition, I will extend my investigation of *miple1* and *miple2* gene expression patterns into the post embryonic stages of development. Particular attention will be focused onto tissues that have been used as model systems for studying signaling pathways that regulate axon guidance, cell migration, and cell proliferation. The data presented in this work will serve as the foundation for future investigations using *Drosophila* as the model organism to understand Midkine and Pleiotrophin function *in vivo*.

Materials and Methods

In situ hybridization for mRNA expression

Embryos were dechorionated in 50% bleach, fixed for 30 minutes in 4% formaldehyde (Polysciences) in PBT (130 mM NaCl, 7 mM Na_2HPO_4, 3 mM KH_2PO_4, 0.1% Triton X-100 v/v) and heptane, devitellinized, and equilibrated in PBT prior to *in situ* hybridization. Larval and adult structures were dissected out in PBT and fixed as described above. The specimens were subsequently washed in PBT, equilibrated in wash buffer (5x SSC, 50% formamide), and prehybridized in hybridization buffer (50% formamide, 5x SSC, 100μg/ml sonicated salmon sperm DNA, 50 μg/ml heparin, 0.1% Tween) at 58°C for 3 hours. *In situ* hybridization was carried out overnight at 58°C using digoxigenin-labeled riboprobes. On day 2, the samples were washed extensively in wash buffer and re-equilibrated in PBTA (PBS, 0.1% Triton-X100, 0.1% bovine serum albumin). Pre-absorbed alkaline phosphatase-conjugated mouse anti-digoxigenin antibody (Roche) was added to the samples at 1:2000 dilution and incubated at 4°C overnight. Signal was amplifed using 4-nitroblue tetrazolium chloride plus X-phosphate (NBT, BCIP, Roche). Images were captured using Zeiss Axioskop 2 with Nomarski optics.

Digoxigenin-labeled riboprobes were generated using *in vitro* transcription. DNA templates for *in vitro* transcription were prepared by PCR amplification of ResGen clone RH10518 for *miple1*, and ResGen clone RE39332 for *miple2*. Primer sequences for *miple1* were left primer 5'-aattctaatacgactcactatagggagcagaagtcgcaccatgagaa-3', and right primer 5'-attaaccctcactaaagggaacgggcttgcagttcttcttga-3'; primer sequences for *miple2* were left primer 5'-aattctaatacgactcactatagggagagccctaagaaggccaattc-3', and right

primer 5'-attaaccctcactaaagggaaccaagaccaacatgcgttcac-3'. The primers contain T3 and T7 RNA polymerase binding sequences for sense and antisense probes, respectively. PCR products were gel purified, phenol chloroform extracted, ethanol precipitated and quantified. *In vitro* transcription was carried out using 2 μg template, 10x DIG Labeling Mix (Invitrogen), T7 (Invitrogen) or T3 (Promega) RNA polymerase incubated for 2 hours at 37°C. A 5-minute bicarbonate treatment at 65°C was performed on antisense *mipple2* riboprobe. Probes were precipitated, resuspended in hybridization buffer, and used at 1:1000 dilution.

Negative controls used for *in situ* hybridization in the embryo are *mipple1* and *mipple2* sense riboprobes hybridized against wild type embryos. For analysis of post embryonic expression, specimens harvested from *mipple1* or *mipple2* mutants were hybridized in the same reaction as wild type. *mipple2*-null flies were generated by crossing deficiency lines *Def(3L)BSC125* (Bloomington Stock number 9290) and *Def(3L)BSC126* (Bloomington Stock number 9291). Homozygous *mipple1*^{c05178} flies (Harvard Stock number c05178) were used as negative controls for *mipple1 in situ* hybridization.

Generation of rabbit antiserum

A 17-amino acid custom synthesized peptide (Global Peptide Services) with the sequence GEVWEEDDHEVLIRNER that corresponds to the amino acid residues 50-66 within the amino terminal loop of Mipple1 was used as the epitope for generating rabbit antisera. One hundred micrograms of peptide dissolved in Freund's complete adjuvant (Sigma) was used for primary injection into 5-week-old female rabbits, followed by three additional boosts spaced 3 weeks apart using 100 μg of the peptide in Freund's

incomplete adjuvant (Sigma). Two weeks after each booster injection, 15 ml of blood was drawn from each rabbit in test bleeds. Epitope recognition was established by detection of HA-tagged Miple1 protein expressed in 293T cells using antisera at 1:1000 dilution, and by positive immunostaining of the native Miple1 protein in wild type *Drosophila* embryos. Rabbits were exsanguinated after the third test bleed.

Specificity of the antiserum was determined by overnight preabsorption of the antiserum at 1:50 dilution in PBTA (PBS + 0.1% Triton X-100, 0.1% bovine serum albumin) with excess amounts of the custom peptide described above prior to immunostaining wild type embryos. .

Immunohistochemistry

Dechorionated, fixed, and devitellinized embryos were washed in PBT and blocked for at least 1 hour in PBTA containing 5% normal goat serum prior to overnight antibody incubation. Larval and adult tissue were dissected in PBT, fixed in 4% paraformaldehyde for 30 minutes, and blocked as described above. Antibody dilution factors are as follows: rabbit anti-Miple1 1:500 (embryos) and 1:100 (larval tissue). The specimens were washed for at least 2 hours in PBTA, incubated with secondary antibody for 2 hours at room temperature followed by 2 more hours of washing in PBTA. All secondary antibodies were used at 1:200 dilution. For DAB amplification of the signal, samples were incubated for one additional hour in the Vecta Stain (Vector Laboratories) reagent prior to development.

DAB-stained samples were cleared in methylsalicylate, and images were captured on a Axioskop 2 microscope using Nomarski optics. For immunofluorescent microscopy, samples were cleared in Slow Fade Gold (Invitrogen) prior to imaging.

RT-PCR

Embryos or tissues were homogenized in Trizol reagent (Sigma), and total RNA was isolated using the manufacturer's protocol. RNA was treated with Rnase-free DNase I (Roche), phenol chloroform extracted twice, sodium acetate precipitated and quantified. Reverse transcription-polymerase chain reaction (RT-PCR) was performed using the SuperScript One-Step RT-PCR System from Invitrogen, and 25 nanograms of total RNA was used for each reaction. Transcripts for *mipple1* were amplified using primer pairs 5'-cagaagtcgcaccatgagaa-3' and 5'-cctttgcgagcagctttatc-3'; for *mipple2* primer pairs 5'-ggctctgcacctagttttgg-3', 5'-ccgtgttgttttcctccact-3'; for *bcd* primers pairs 5'-tcagcagcagcaataccatc-3' and 5'-cgtgcattgatattggttcg-3'; for *actin5C* primers pairs 5'-cgttctggactccggcgatgg-3' and 5'- gtacttgcgctctggcggggc-3'. All primer pairs spanned an intron such that amplification of contaminating genomic DNA could be distinguished from the RT-PCR amplified products. The RT step was performed at 50°C for 30 minutes followed by 36 to 40 cycles of PCR in a 50 μl reaction. Cycling conditions are as follows: 95°C for 30 seconds, 55°C for 30 seconds, and 72°C for 1 minute. PCR products were resolved by 1.5% agarose gel electrophoresis.

Results

Embryonic expression of *miple1* and *miple2*

miple2

I used *in situ* hybridization with antisense *miple2* riboprobes to investigate *miple2* mRNA expression in the *Drosophila* embryo. My results confirm that *miple2* is expressed in the endoderm and the mesoderm during embryogenesis. I detected no tissue specific distribution of the *miple2* mRNA prior to gastrulation. The *miple2* message is first observed during stage 8, as the embryo undergoes germband extension. Tissues surrounding the stomodeum and the proctodeum exhibit strongest staining (Figure 2.1A, B, C). As the germ band contracts, the domains of *miple2* expression expands caudally from the stomodeum and rostrally from the proctodeum (Figure 2.1D, E). The two domains ultimately converge at the midgut by the end of germ band retraction at stage 12 (Figure 2.1F). The dynamic patterns of *miple2* mRNA distribution during these stages of development suggest that gene is expressed in the endodermal tissues that make up the anterior and posterior midgut primordium (AMG and PMG), which migrate as mesenchymal masses to enclose the yolk cells during gut formation.

As the midgut expands and undergoes constriction, *miple2* message is distributed in tissues that line the gut (Figure 2.1G, H, I). In addition, tissues lining the foregut and the hindgut also express *miple2*. By the end of embryogenesis at stage 17, cells express the *miple2* message form a continuous lining of tissues along the entire embryonic gut.

In addition to the endoderm, I observed *miple2* expression in the mesoderm. Beginning in stage 8, a continuous, a thin sheet of *miple2* expressing cells is visualized along the entire length of the germband (Figure 2.1A-C, arrowheads). By stage 11,

miple2 expressing cells are detected as a band of tissue underlying the migrating anterior and posterior midgut primordium (Figure 2.1A-D, arrowheads). This tissue corresponds to the visceral mesoderm.

Taken together, my data indicate that *miple2* is expressed in both the endoderm and the mesoderm during embryogenesis. In addition, the persistence of the *miple2* message in the endoderm throughout embryogenesis suggests that *miple2* expression is associated with both the mesenchymal and epithelial forms of endoderm during embryogenesis.

miple1

I investigated embryonic *miple1* expression at the levels of mRNA and protein. My situ hybridization results suggest that embryonic *miple1* mRNA expression is primarily localized to the central nervous system. The *miple1* message is first detected in the developing ventral nerve cord (VNC) at the end of germ band extension at stage 12 (Figure 2.2C). Progressively stronger signals are observed in the VNC during subsequent stages (Figure 2.2D-G). I first detected *miple1* message in the brain at stage 14 (Figure 2.2E, arrowhead). Strong expression of *miple1* mRNA persists in both the brain and the VNC to the end of embryogenesis (Figure 2.2F-H).

A closer examination of *miple1* expression within the central nervous system suggests that *miple1* is expressed in the glia cells. In the VNC, *miple1* message is first detected in a single cluster of cells in each parasegment at the ventral midline beginning in stage 15, with additional staining in the longitudinal fascicles (Figure 2.3A, C). By stage 16, two additional clusters of cells located anterolaterally to the midline cells also express *miple1* (Figure 2.3B, D). These findings are corroborated by my

immunohistochemical findings using rabbit anti- Miple1 antisera. Stage 15 embryos show a single midline cell immunoreactive against rabbit anti-Miple1 antisera. Three additional cell clusters located in the longitudinal fascicles stain positive for Miple1. The processes extending from these cells are also stained (Figure 2.3E, I, J). By stage 16, Miple1 expressing cells in each parasegment consist of a single cell located at the midline and associated with the posterior commissure, clusters of cells located at the junctions of the anterior commissures and the longitudinal fascicles, and three more cell clusters located in the longitudinal fascicles (Figure 2.3L). Processes from these cells stain positive for Miple1, and these processes are associated with the the commissures, the longitudinal fascicles, as well as projections defasciculating from the longitudinal fascicles to the periphery. Based on the positions of the cell bodies in relation to the commissures and fascicles during CNS development, I conclude that the cells that express Miple1 most likely correspond to the midline glia middle (MGM) and longitudinal glia 1-6 (LG1-6)[106, 107].

In addition to the central nervous system, I have also detected *miple1* mRNA in the mesoderm and the endoderm. The distribution of *miple1* mRNA in the endoderm and the mesoderm closely parallels that of *miple2* (Figure 2.2A-F). However, Miple1 protein distribution was not detected in these tissues based on immunohistochemical staining.

Maternal contribution of *miple1* and *miple2*

Since I was unable to detect tissue specific distribution of either *miple1* or *miple2* prior to gastrulation using *in situ* hybridization, I performed RT-PCR on total RNA isolated from one-hour-old embryos. My results indicate that both *miple1* and *miple2*

messages are present during the first hour after egg laying, prior to the onset of zygotic transcription (Figure 2.4). These findings suggest that both *mipple1* and *mipple2* are maternal genes.

Larval expression of *mipple1* and *mipple2*

mipple2

I employed *in situ* hybridization to characterize *mipple2* mRNA expression in late stage, 3rd instar larvae. Specific staining is detected in all of the imaginal discs: eye-antenna, labial, wing, haltere, leg, and genital discs, as well as the brain (Figure 2.5A-G). The distribution pattern of *mipple2* mRNA in all of the tissues is diffuse and uniform.

mipple1

mipple1 mRNA expression as determined by *in situ* hybridization demonstrates CNS specific expression of *mipple1* during the late larval stage. The mushroom body and the thoracic neuromeres within the ventral ganglion stain positive for *mipple1* (Figure 2.6A).

I was unable to detect higher-than-background levels of *mipple1* in the imaginal discs using either *in situ* hybridization or RT-PCR (Figure 2.6C). These findings suggest that unlike *mipple2*, *mipple1* expression during the late larval stage is mostly restricted to the central nervous system.

miple1 and *miple2* expression in adult tissues

miple2

I examined selected structures from the adult stage for *miple2* mRNA expression using both *in situ* hybridization and RT-PCR. In the brain, diffuse pattern of *miple2* message distribution is detected at levels significantly higher than background (Figure 2.7A, A'). However, I was not able to determine any tissue specific distribution within the brain.

In situ hybridization demonstrates that the male reproductive system expresses *miple2*. The *miple2* message is visualized in both the testes and the accessory glands (Figure 2.7B). Closer inspection of the testes revealed that the *miple2* message is detected at low levels near the apex of the testis, the site of early stages of spermatogenesis (Figure 2.7C). Progressively more intense staining of *miple2* is visualized toward the base of the testis, with the most intense staining associated with cells at the 64-spermatid cyst stage of spermatogenesis (Figure 2.7D). These findings suggest a positive correlation between the levels of *miple2* expression and the stages of spermatid maturation, with lower levels of *miple2* expresssion at early spermatogenesis and higher levels expressed in more mature spermatids.

I was unable to detect higher-than-background levels of *miple2* expression in the ovary using *in situ* hybridization. However, *miple2* message was detected using RT-PCR (Figure 2.7E). While these findings do not reveal the stage during which *miple2* is expressed during oogenesis, they are consistent with RT-PCR results demonstrating the presence of the *miple2* message in the early embryo.

miple1

In situ hybridization using *miple1* antisense riboprobe detected tissue specific localization of *miple1* in the adult brain (Figure 2.8A). *miple1* mRNA distributes to the cell bodies located within the pedunculus of the mushroom body (Figure 2.8C). Since the pedunculus consists of bundles of neuronal axons, and the only cell bodies within the pedunculus belong to those of the glia, these findings are suggestive that *miple1* is expressed in the glial cells in the adult brain.

I was unable to detect higher-than-background levels of *miple1* in either the testes or the ovaries. RT-PCR results do not indicate that *miple1* is expressed in these tissues (Figure 2.8D).

Discussion – *miple1* and *miple2* expression during *Drosophila* Development

Embryonic expression data suggest that *miple1* is expressed in the glia throughout *Drosophila* neural development. Combined *in situ* hybridization and immunohistochemistry data in the embryo suggest that the onset of Miple1 expression occurs after the formation of commissures and fascicles and the defasciculation of the motor neurons from the CNS. These findings in turn imply that Miple1 unlikely functions as an initial cue for axon guidance during CNS development. Miple1 protein localizes to the axon tracts throughout the VNC and axon projections to the periphery. Based on the premise that Miple1 is expressed in the glia, the localization of the Miple1 protein along the axon tracts in the VNC and projections to the periphery may indicate that Miple1 is associated with the glial processes that ensheath the axons of the maturing neurons. These findings are consistent with observations in mouse embryonic development, in which both Midkine and Pleiotrophin protein localize to the axon tracts and glial processes along axon tracts[79].

While embryonic *miple1* appears to be expressed primarily in the nervous system, *miple2* is expressed in a much broader range of tissues. Data presented in this study suggest that *miple2* mRNA is expressed in both the endoderm and the mesoderm during embryogenesis. The timing of *miple2* expression in both tissues correlates with cell migration. The mesoderm spreads along the overlying ectoderm and migrates dorsally after gastrulation. Simultaneously, the anterior and posterior midgut primordia migrate toward each other from opposite ends of the embryo along the underlying visceral mesoderm in response to a yet undetermined extracellular signal. Based on findings presented in this study, Miple2 is a marker for migrating cells during embryogenesis.

While the expression of *mipple1* and *mipple2* are associated with two entirely different processes during embryogenesis, larval *mipple1* and *mipple2* expression patterns both correlate with cell proliferation. *In situ* hybridization data suggest that *mipple2* is primarily expressed in the imaginal discs, which are epithelial tissues that undergo extensive cell proliferation during the late larval and pupae stages to give rise to adult appendages. As in during embryogenesis, larval *mipple1* expression primarily localizes to the CNS. Regions to which *mipple1* mRNA localizes, including the thoracic neuromeres, the optic anlarge, and the brain proliferative centers, undergo extensive cell division to give rise to neurons that innervate adult tissues. Combined *mipple1* and *mipple2* expression data in the *Drosophila* larvae are consistent with Midkine and Pleiotrophin expression data in mice, in which both proteins localize to the proliferative centers in the embryonic brain[16, 79]. Taken together, my larval expression data suggest that *mipple1* and *mipple2* have potential functions in cell proliferation.

Adult expression data presented in this study also suggest the conservation of Miple1, Miple2, Midkine and Pleiotrophin function. In the adult *Drosophila* brain, *mipple1* mRNA is detected in the pedunculus of the mushroom body. Pleiotrophin protein localizes to the axon tracts of the hippocampal and Purkinje neurons in adult mice[81, 82]. A common theme between the *Drosophila* mushroom body and the mammalian hippocampus and cerebellum is that they all exhibit activity-dependent synaptic plasticity.

My *in situ* hybridization and RT-PCR data suggest that *mipple2* is expressed in both the male and the female gonads in *Drosophila*. Moreover, both *mipple1* and *mipple2* messages have been detected in the early embryo as maternal genes. These findings are

consistent with data from mammalian studies, which suggest a requirement for Midkine and Pleiotrophin in the gonads. Both Midkine and Pleiotrophin are expressed in the uterus[80]. More significantly, *ptn-/-; mk-/-* double mutant mice are female sterile[99]. Furthermore, chimeric male mice carrying a dominant negative allele of Pleiotrophin undergo germ cell apoptosis and have agametic testes[80, 108].

The expression patterns of *miple1* and *miple2* throughout *Drosophila* development as revealed in this study are strikingly similar to the previously published Pleiotrophin and Midkine expression data in mammals. Even more remarkably, the molecules that have been identified as putative Midkine and Pleiotrophin receptors based on *in vitro* biochemical interactions have homologues in *Drosophila*, and studies in the past have demonstrated that they are required in the development of tissues in which both *miple1* and *miple2* are expressed.

Among the list of putative receptors is a class of extracellular molecules known as heparan sulfate proteoglycans (HSPGs). All HSPGs consist of a protein core to which heparan sulfate (HS) glycosaminoglycan (GAG) chains are attached. HSPGs with a transmembrane protein core are known as Syndecans; the protein core of Glypican is attached to the plasma membrane via a glycosylphosphatidylinositol (GPI) anchor. Biochemical binding assays have identified Syndecans and Glypicans as putative receptors for Midkine and Pleiotrophin[61-63].

In *Drosophila*, *sdc* encodes the single Syndecan homologue, and *dally* and *dally-like protein* (*dlp*) encode the two Glypican homologues[109-111]. Syndecan is expressed in the embryonic CNS, while Dally and Dlp expression overlap with *miple2*. Developmental and genetic data have demonstrated HSPGs as key components in mediating cell-cell

signaling. *dally* and *dlp* mutants have wing phenotypes resembling those of mutants with disruptions in Wingless/Wnt, Hedgehog, Decpapentaplegic/TGFβ, and FGF signaling[110, 112-117]. Phenotypic analyses in the embryo have also demonstrated overlapping functions of Dally and Dlp in Hedgehog-dependent segmental polarity patterning in the ectoderm[118]. Since Midkine and Pleiotrophin bind Syndecans and Glypican *in vitro*, it is possible that Miple1 and Miple2 have required function as extracellular components in signaling pathways that require HSPG function, including Wingless/Wnt, Hegehog, Dpp/TGFβ, and Fibroblast Growth Factor (FGF) signaling pathways.

In addition to HSPGs, biochemical binding assays have identified receptor protein tyrosine phosphatase β, also known as tyrosine phosphatase ζ (RPTPβ/PTPζ), as a putative receptor for both Midkine and Pleiotrophin, and that the binding of Midkine or Pleiotrophin inactivates RPTPβ/PTPζ phosphatase activity[11, 12, 52]. The inhibitory effect has been proposed to maintain the tyrosine phosphatase substrates in the phosphorylated, active state, which is correlated with neurite extension and cell migration.

The *Drosophila* genome encodes six RPTP homologues. Five of the six homologues, DPTP10D, DLAR, DPTP52F, DPTP69D, and DPTP99A, are expressed in the embryonic central nervous system[119-124]. Mutants in this group of "neural RPTPs" exhibit defects in neural development, ranging from commissure formation and collapse of longitudinal fascicles in the ventral nerve cord to motor axon targeting defects in the periphery. Expression pattern analysis of *dptp4E* mRNA suggests that it is expressed in the embryonic endoderm and mesoderm, at the same time *miple2* is expressed. In addition, *dptp4E* message is also detected in the ventral midline cells in the CNS. To date, no *dptp4E* mutant phenotype has been characterized.

All of the *Drosophila* RPTPs except DLAR are orphan receptors. Multiple proteins have been demonstrated to bind RPTPs *in vitro*, yet to date only two molecules, the HSPGs Syndecan and Dally-like protein (Dlp), have been demonstrated as *in vivo* ligands for DLAR[125, 126]. Combined tissue culture findings and our expression data suggest that Miple1 and Miple2 may be RPTP ligands. Miple1 may function to stabilize the axon projection by turning off the RPTP signal after initial growth cone pathfinding is completed. Alternatively, Miple1 may bind Sdc or Dlp as a cofactor to sequester the activating ligands from the RPTPs, thereby inactivating the receptors. A similar role may be played by Miple2 in the embryonic mesoderm and endoderm in regulating DPTP4E signaling as cells migrate. Recent data from a study in which ectopic overexpression of *miple1* in the embryonic mesoderm produced a cell migration defect resembling the phenotype of mutants with hyperactive Heartless FGF receptor signaling are consistent with this hypothesis[127].

Anaplastic lymphoma kinase (ALK), a receptor tyrosine kinase and proto-oncogene, has also been identified as a potential receptor for Midkine and Pleiotrophin in biochemical binding assays[25, 28]. During embryogenesis, *Drosophila* ALK (Alk) is expressed in the visceral mesoderm and the central nervous system, sites of respective *miple2* and *miple1* expression[128]. However, genetic and developmental data suggest that Jelly belly (Jeb), a secreted molecule with no structural resemblance to Miple1 and Miple2, as the biological ligand for Alk[129, 130]. Nevertheless, the possibility that Miple1 and Miple2 may function as cofactors for Alk signaling cannot be excluded. One possibility is that Miple2, in conjunction with the HSPGs, act to modulate Jeb signaling by regulating its extracellular distribution.

The most straightforward approach to testing the proposed functions and identifying the receptors of Midkine and Pleiotrophin in a living system involves the generation of loss-of-function mutants and the analyses of the mutant phenotypes. Data presented in this chapter suggest that *Drosophila* is a logical model system, given the high degree of conservation between Miple1, Miple2, Midkine, and Pleiotrophin in multiple biological processes throughout development. In addition, allelic series of mutations in genes encoding components of the signaling pathways in *Drosophila* are publicly available. They are useful reagents for investigating potential genetic interactions between the *miple1*, *miple2*, and the genes encoding components of the signaling pathways. *Drosophila* development with respect to signaling has been thoroughly characterized. Therefore, correlation between any developmental phenotype observed in the embryo or the wing in *miple1* and *miple2* mutants will allow for the assignment of Miple1 and Miple2 to the known signaling pathways. The combination of genetic amenability and the power of phenotypic correlation, in addition to the remarkable conservation of Miple1, Miple2, Midkine, and Pleiotrophin in developmental processes, make *Drosophila* an ideal choice for studying Midkine and Pleiotrophin function *in vivo*.

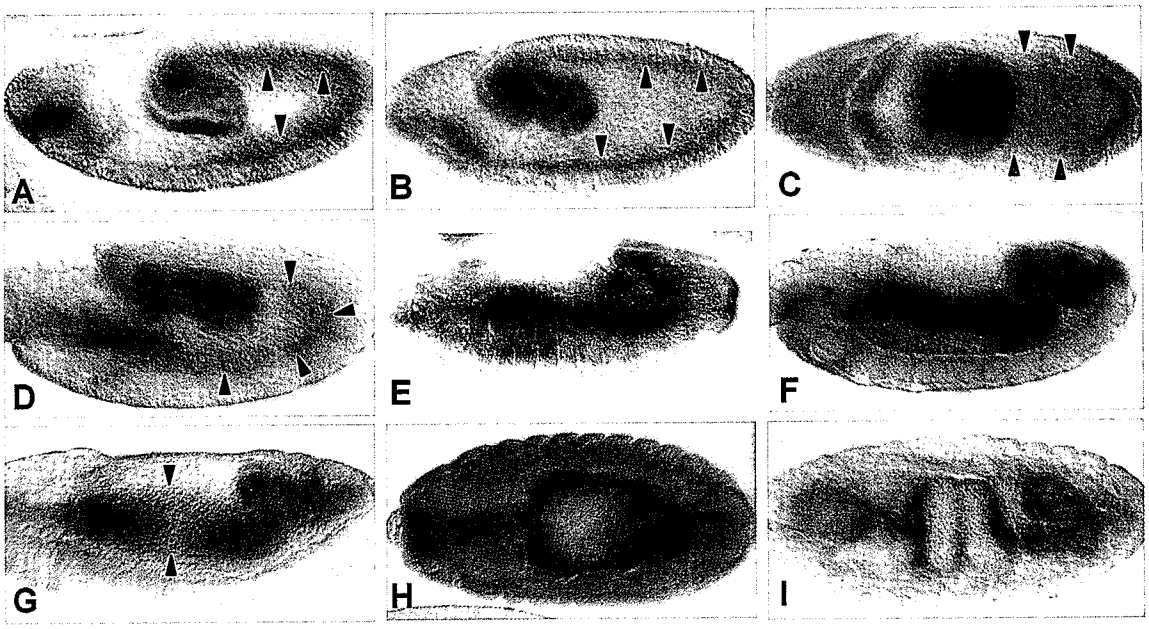

Figure 2.1. Embryonic expression patterns of *miple2*.
Whole mount embryos hybridized with *miple2* antisense riboprobe followed by alkaline phosphatase reaction. Anterior is to the left. (A) Early stage 8. *miple2* message is first detected in the stomodeum and proctodeum. There is also light staining in the mesoderm (arrowheads). Lateral (B) and overhead (C) views of late stage 8 embryos. The mesoderm is stained as a sheet of tissue along the entire germband. (D) Lateral view of a stage 11 embryo at the beginning of germband retraction. The *miple2* domain at the stomodeum extends caudally, and the proctodeum *miple2*-staining domain extends rostrally along the underlying visceral mesoderm, which is also stained (arrowheads). (E) Stage 12 embryo. The anterior and posterior domains of *miple2* expression begin to merge. (F) Stage 13 embryo. *miple2* is now expressed along the entire gut. (G) Stage 14 embryo. *miple2* is expressed along the entire embryonic gut, including the lining of the midgut undergoing the first constriction (arrowheads). (H) Overhead view of a stage 15 embryo. *miple2* staining is present at the foregut and hindgut, and the lining of the first midgut constriction. (I) Overhead view of a stage 16 embryo. The foregut, hindgut, and the lining of the midgut show *miple2* staining.

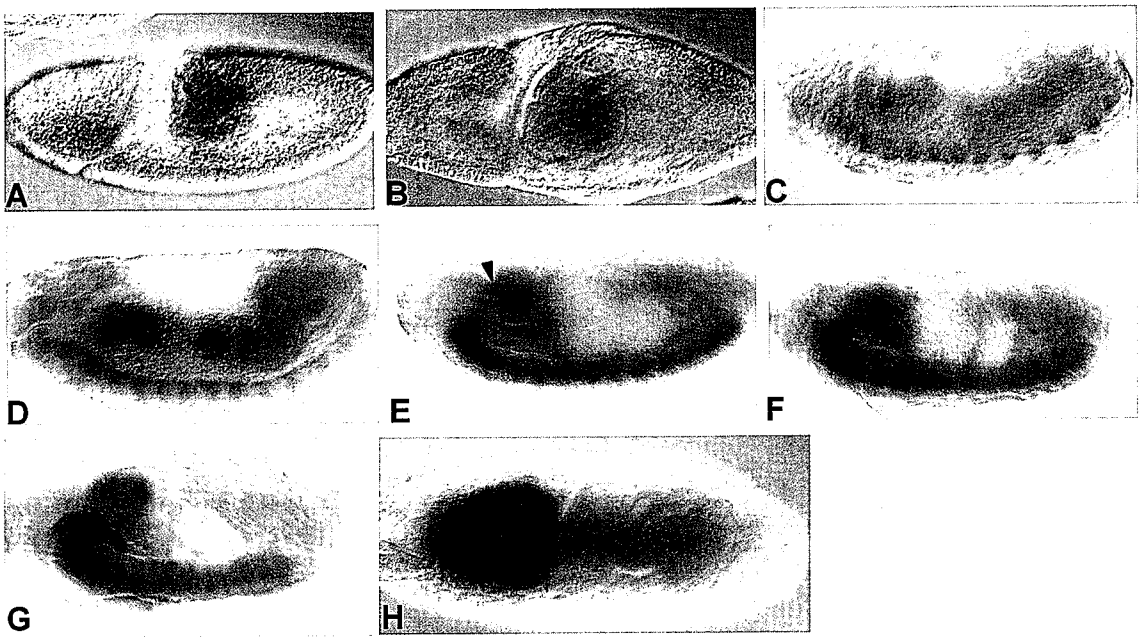

Figure 2.2 Embryonic expression of *miple1* mRNA.
Whole mount embryos hybridized with *miple1* antisense riboprobe followed by alkaline phosphatase reaction. Anterior is to the left. Lateral (A) and dorsal (B) views of stage 8 embryos. *miple1* message is detected in the stomodeum and the proctodeum. Light staining is also seen in the mesoderm. (C) Lateral view of a stage 13 embryo, showing *miple1* expression in the endoderm and the central nervous system. (D) Stage 14 embryo. *miple1* staining is present in the tissues lining the endoderm; the ventral nerve cord (VNC) also stains positive for *miple1*. (E) Stage 15 embryo showing *miple1* staining in both the VNC and the brain (arrowheads). *miple1* message is also seen in a thin layer of tissues surrounding the midgut. (F) Stage 16 embryo showing positive *miple1* staining in the brain, the VNC, and midgut linings. Later (G) and dorsal (H) views of a stage 17 embryo. The brain and the VNC stains prominently for *miple1*; signal in the gut is no longer detectable.

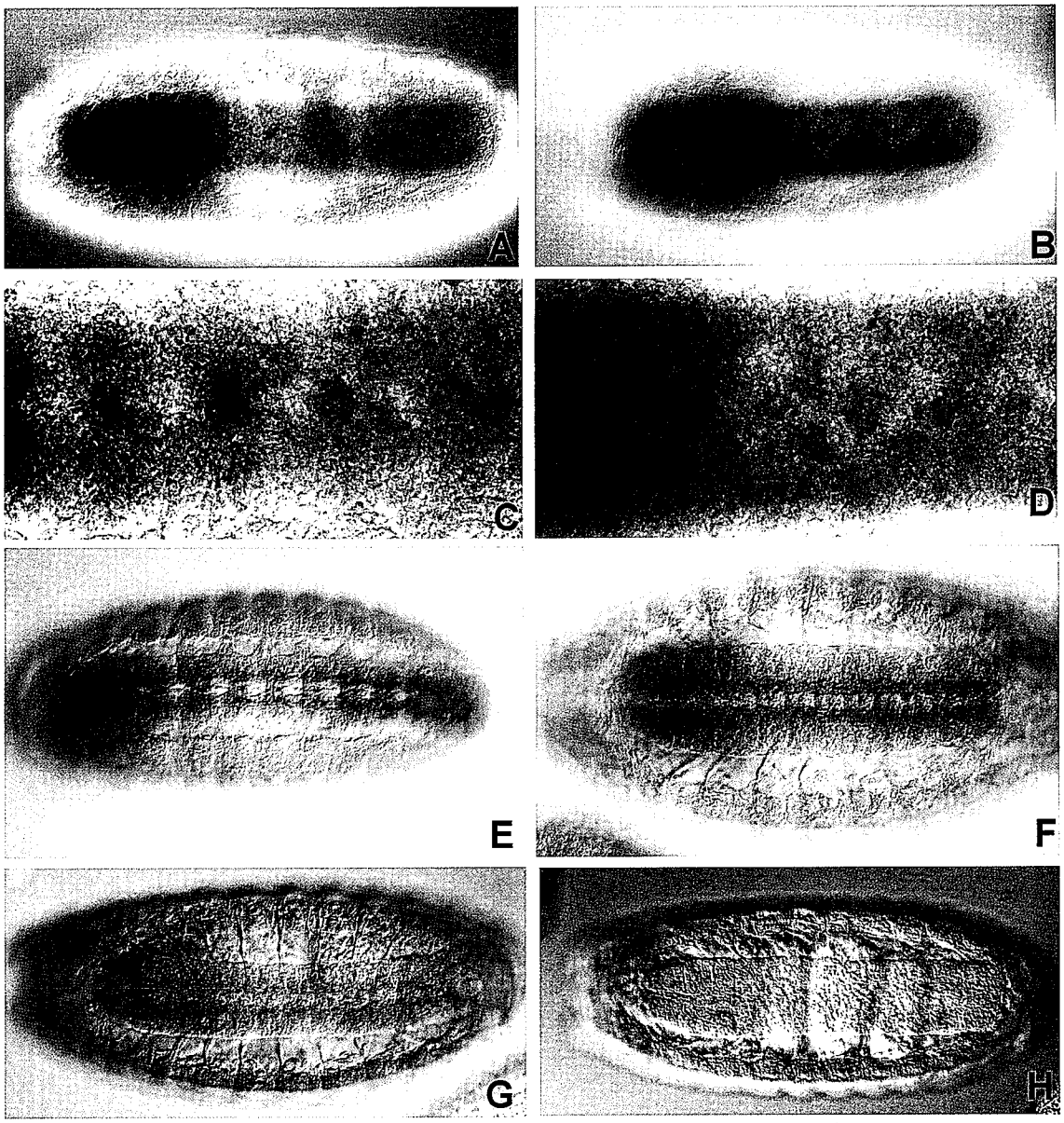
A
B
C
D
E
F
G
H

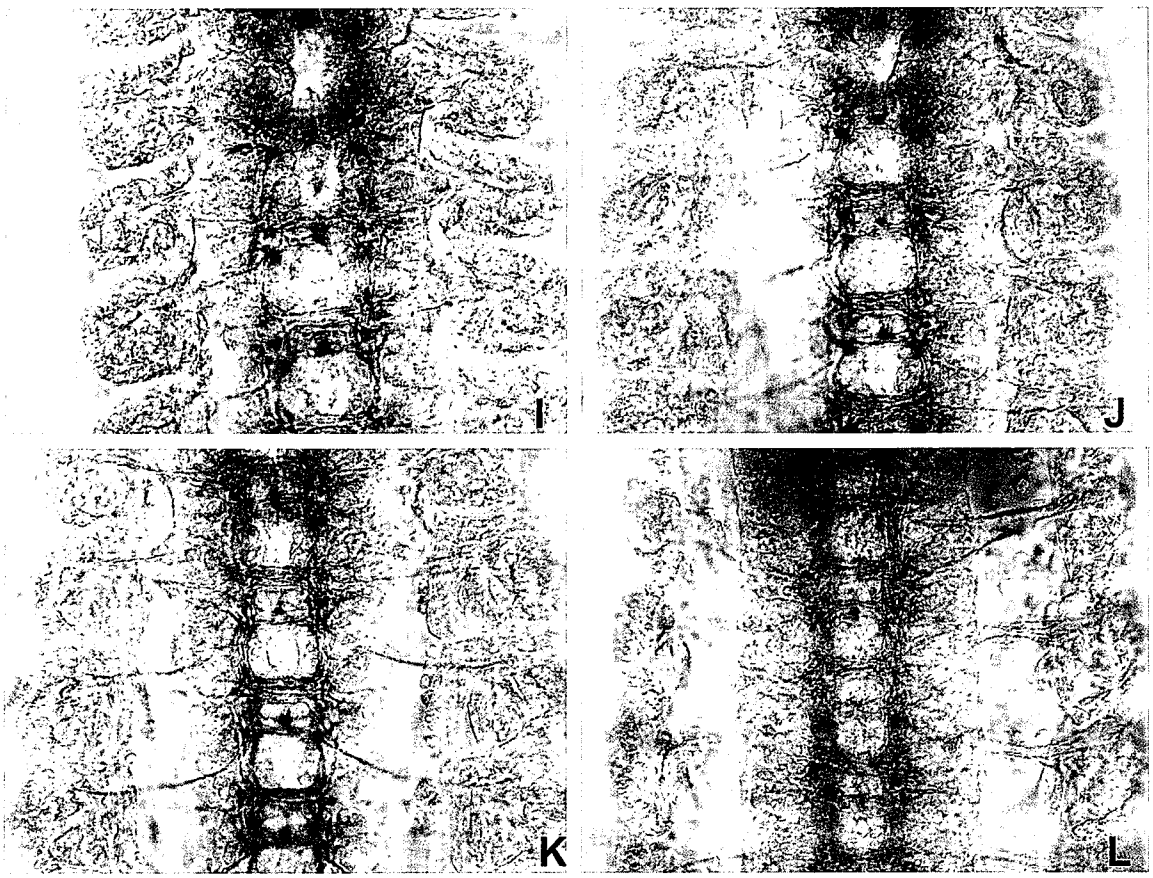

Figure 2.3. Distribution of *miple1* mRNA and Miple1 protein in the embryonic central nervous system.

(A-F) Whole mount embryos, anterior is to the left. Low (A) and high (C) magnifications of a stage 15 embryo hybridized with *miple1* antisense riboprobe. *miple1* message is localized to a single cluster of cells at the midline of the ventral nerve cord. *In situ* hybridization of a late stage 16/early stage 17 embryo at low (B) and high (D) magnification. A single cluster of *miple1* expressing cells is located at the midline, and two additional clusters of cells located anterolaterally show positive *miple1* staining. *miple1* message is also visible in longitudinal fascicles.

(E-L) Immunohistochemistry of embryos stained with rabbit anti-Miple1 antiserum. Ventral views of embryo at stage 15 (E). Miple1 immunoreactivity is restricted to a single cluster of cells at the ventral midline, with additional cell clusters located within the fascicles. The commissures and fascicles also demonstrate diffuse staining for Miple1. (F) Stage 16 embryo. Positive Miple1 immunostain is detected in the ventral nerve cord as well as projections to the periphery. A single cluster of Miple1 staining cells is located at the midline and associated with the posterior commissure. Two additional clusters are located anterolaterally at the juncture between the anterior commissure and the fascicles. More Miple1 expressing cells are found in the longitudinal fascicles.

(G, H) Specificity of the anti-Miple1 antisera. Immunostains of stage 17 embryos incubated with anti-Miple1 antisera preabsorbed with bovine serum albumin (BSA) (G) or BSA and oligopeptide with sequence corresponding to amino residues 50-66 of

Miple1 (H). CNS-specific immunoreactivity is present in embryos incubated with BSA-treated Miple1 antisera (G); immunoreactivity is absent in embryos incubated with antiserum preabsorbed with Miple1 oligopeptide (H).
(I-L) High magnifications of embryos immunostained with rabbit anti-Miple1 antisera. Anterior is up. (I) Early stage 15 embryo showing a single cluster of Miple1-expressing cell at the midline, with an additional three clusters of cells staining positive for Miple1 in the fascicles. (J) Mid stage 15 embryo showing the localization of the Miple1 staining cell between the separating anterior and posterior commissures. (K) Late stage 15 embryo. The commissures and fascicles are now immunoreactive against Miple1 antiserum. In addition, positive immunostain is also visualized in the projections to the periphery. (L) Stage 16 embryo. Commissures, fascicles, and peripheral projections stain positive for Miple1. Cell bodies immunoreactive against Miple1 are seen in a single midline cell associated with the posterior commissure, and in three additional clusters in the longitudinal fascicles.

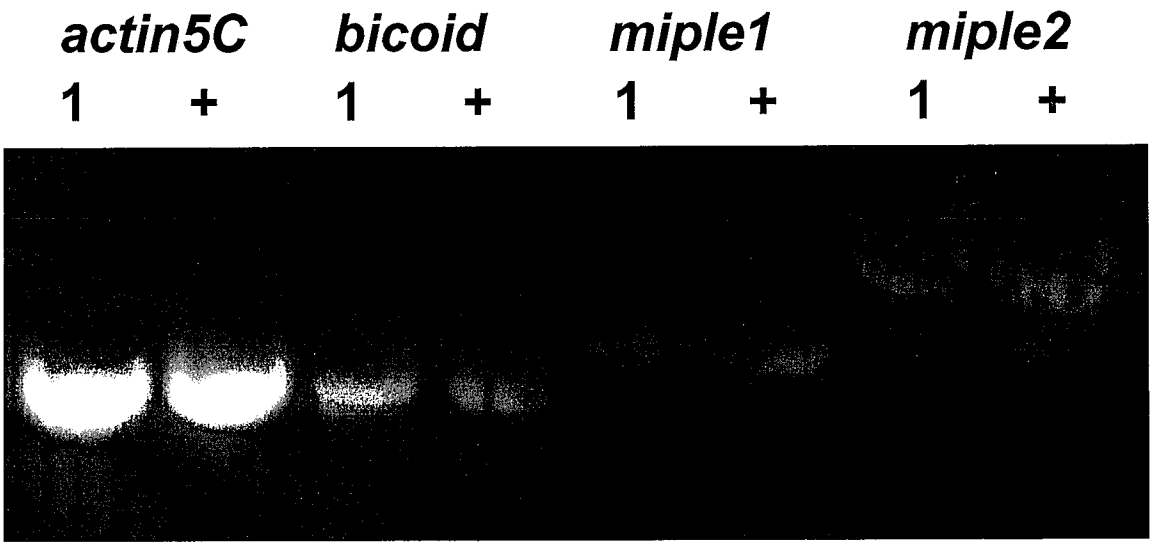

Figure 2.4. *miple1* and *miple2* messages are present in the early embryo.
RT-PCR results using 25 nanograms of total mRNA isolated from one-hour (1) and 16-hour (+) embryo collections amplified for 40 cycles. *actin5C* is the loading control, and *bicoid* is the positive control for maternal genes. Both *miple1* and *miple2* messages are detected in one-hour-old embryos collections.

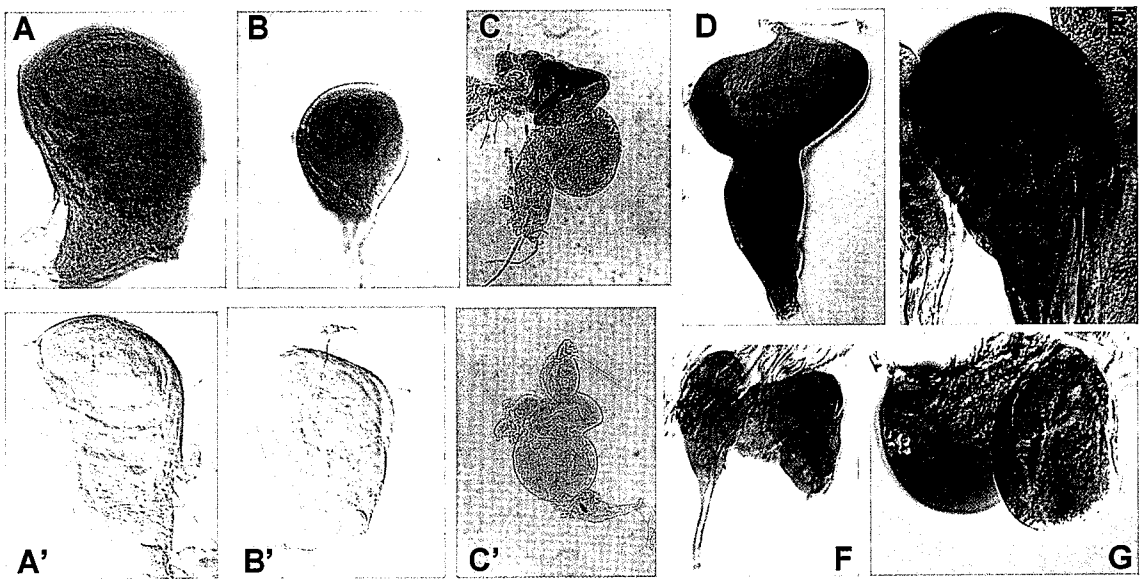

Figure 2.5. *miple2* mRNA expression in the late larval stage.
Whole mount images of larval imaginal discs hybridized with *miple2* antisense riboprobe followed by alkaline phosphatase reaction. Wing disc isolated from wild type (A) and *miple2* mutant (A') 3rd instar larvae. Diffuse staining observed in wild type, but not in the wing imaginal disc. Similar patterns of specific *miple2* staining are also observed in the leg disc (B), eye-antenna disc and the brain (C) obtained from wild type but not *miple2* mutant (B' and C') larvae. Additional *miple2* message is also detected in wild type eye-antenna (D), haltere (E), labial (F), and gonadal (G) imaginal discs.

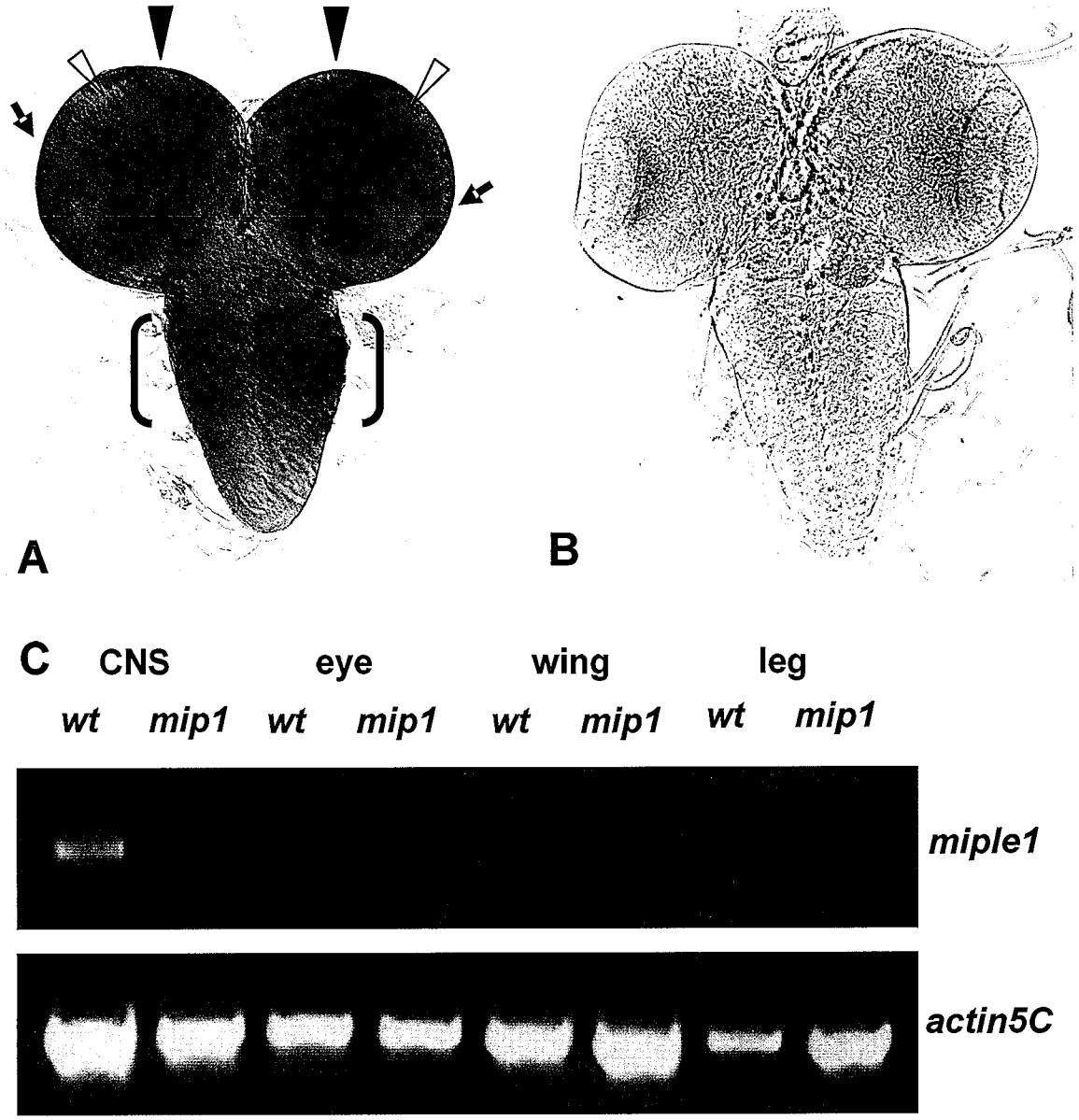

Figure 2.6. *miple1* expression in the third instar larvae.
(A) Wild type and (B) *miple1* mutant, negative control larval brains from the same *in situ* hybridization reaction. Regions within the hemispheres that stain specifically for the *miple1* message include the mushroom bodies (closed arrowheads), the proliferating neuroblasts within the hemispheres (open arrowheads), and the optic lobe anlargen (arrows). In addition, the thoracic neuromeres in the ventral ganglion also stain positive for *miple1* (brackets).
(C) RT-PCR results using 25 nanograms of total RNA isolated from tissues of third instar wild type (*wt*) and *miple1* mutant (*mip1*) larvae after 35 cycles of amplification. *actin5C* is the loading control. *miple1* message is detected in the wild type CNS (brain and ventral ganglion). Specific *miple1* expression is not detected in the wild type eye, wing, and leg imaginal discs.

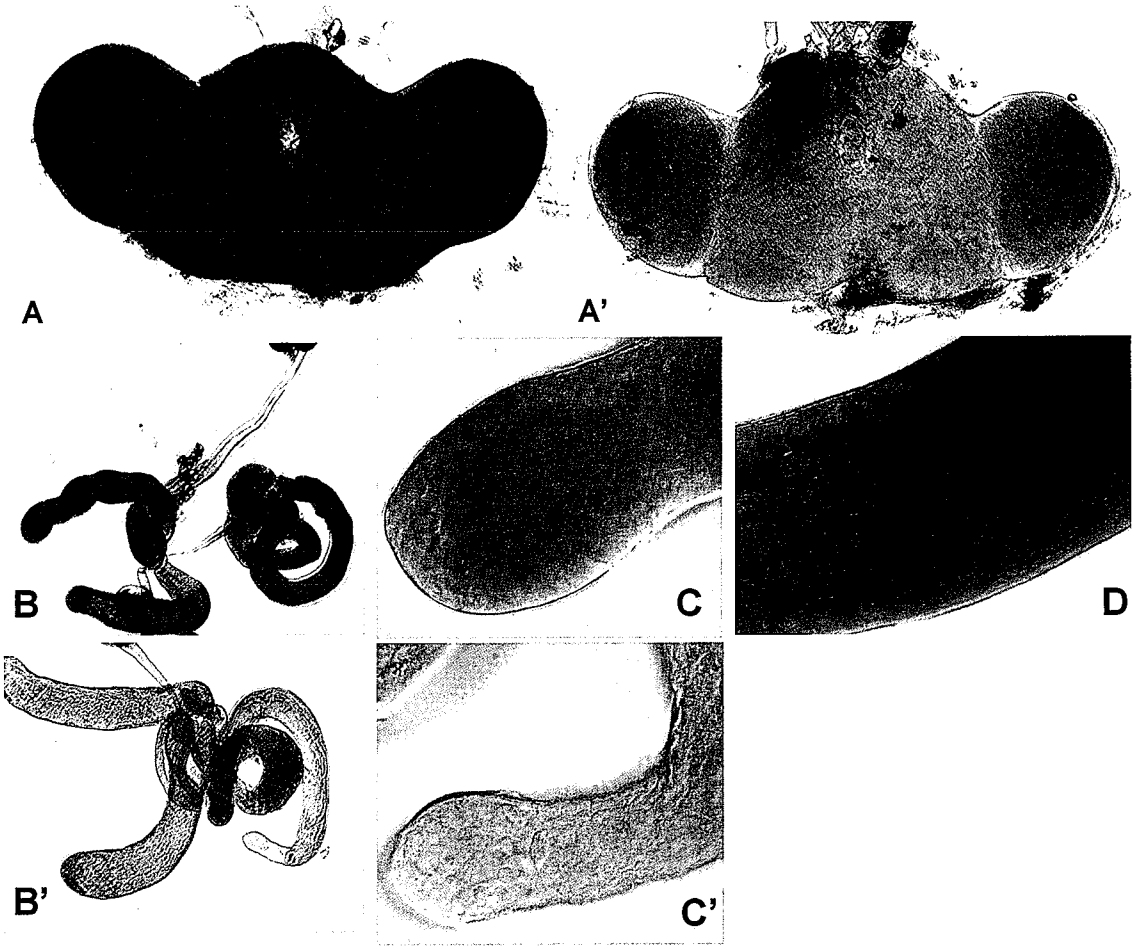
A
A'
B
C
D
B'
C'

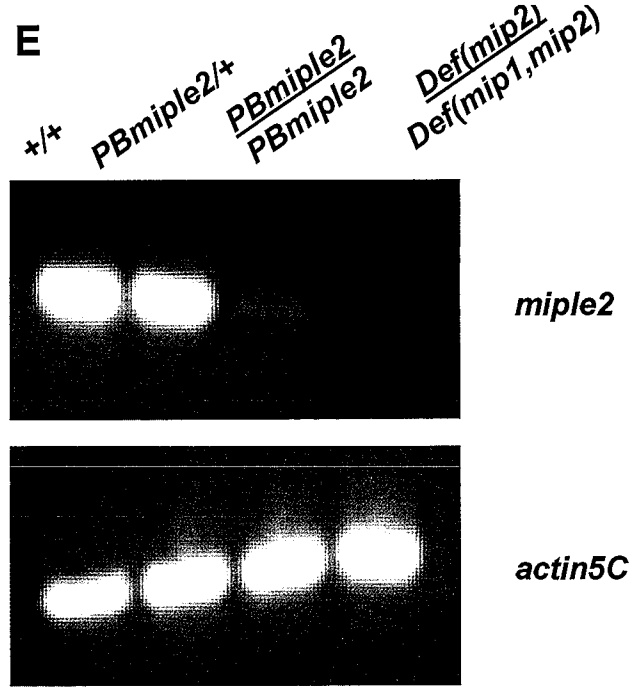
E
+/+
PBmiple2/+
PBmiple2
PBmiple2
Def(mip2)
Def(mip1,mip2)
miple2
actin5C

Figure 2.7. *miple2* expression in selected adult structures.
Whole mount images of adult structures hybridized with *miple2* antisense riboprobe. Wild type (A) and *miple2*-null (A') brains from the same reaction. Diffuse, specific staining is detected throughout the adult brain. Wild type (B) and *miple2* mutant (B') male genitalia. Specific *miple2* message is detected in both the testis and the accessory glands of the wild type male genitalia. High magnification images of the apex of the testis showing the presence of the *miple2* message in wild type (C) but not mutant (C') tissue. (D) Higher magnification of an image taken from the middle of the testis showing diffuse *miple2* staining in the middle of the testis. (E) RT-PCR of total RNA isolated from wild type, *piggyBac-miple2* heterozygous, homozygous *piggyBac-miple2*, and *miple2*-null (*Def(mip2)/Def(mip1, mip2)*) adult female ovaries. *actin5C* is used as loading control. Lower levels of *miple2* message is observed in females homozygous for the *piggyBac-miple2* allele, and no message is detected in the *miple2*-null ovaries.

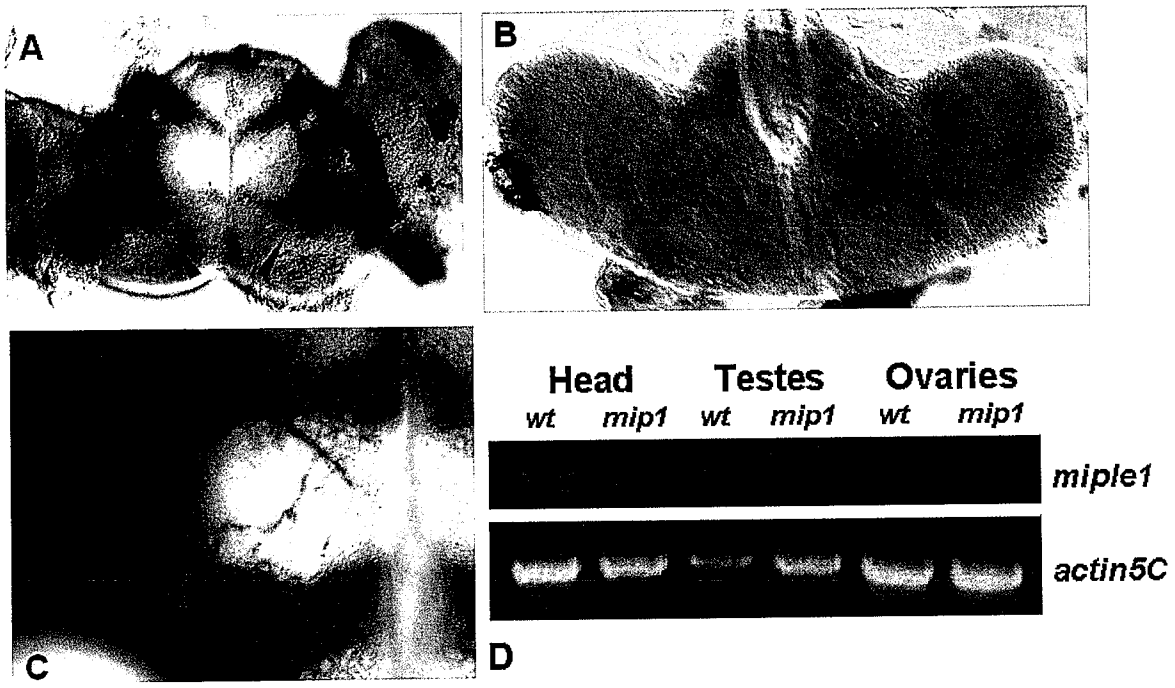

Figure 2.8. *miple1* expression in selected adult organs.
Whole mount images of adult brains hybridized with *miple1* antisense riboprobe. Specific staining is visualized in the mushroom body pedunculus (arrow heads) of wild type (A) but not *miple1* mutant (B) brains from the same *in situ* hybridization reaction. (C) Higher magnification of a wild type adult brain showing cell bodies within the pedunculus staining positive for the *miple1* message.
(D) RT-PCR results using 25 nanograms of total RNA isolated from wild type (*wt*) and *miple1* mutant (*mip1*) adult flies after 35 cycles of amplification. *actin5C* is the loading control. Specific *miple1* message is detected in the adult head, but not in the testes or ovaries.

Chapter 3

Characterization of *miple2*-null mutant

Abstract

Midkine and Pleiotrophin are secreted molecules that elicit a wide variety of responses in tissue culture, including cell proliferation, survival, neurite outgrowth, branching morphogenesis, and migration. Biochemical approaches have identified multiple molecules as putative receptors through which Midkine and Pleiotrophin exert their signaling effects. Miple1 and Miple2 are the homologues for Midkine and Pleiotrophin in *Drosophila*. In this study, I used loss-of-function *miple2* mutant to investigate the potential role of Miple2 as a cofactor in Anaplastic Lymphoma Kinase (Alk) signaling. Developmental and genetic interaction data presented in this chapter do not establish the requirement of Miple2 in Alk signaling. Results from phenotypic analyses are inconclusive for determining Miple2 as a required cofactor in morphogen signaling in the larval wing imaginal disc. I also report a potential male sterile phenotype secondary to defective sperm individualization in *miple2*-null flies.

Introduction

Midkine and Pleiotrophin are secreted, heparin-binding small molecules with proposed signaling functions. Biochemical binding assays have identified multiple transmembrane molecules as potential receptors for Midkine and Pleiotrophin. In tissue culture experiments, Midkine and Pleiotrophin promote neurite outgrowth, cell migration, branching morphogenesis, cell proliferation, and cell survival. To date, phenotypic analyses of loss-of-function Midkine and Pleiotrophin mutants in mice have been unable to uncover the *in vivo* function of these molecules.

Midkine and Pleiotrophin are conserved across the metazoan kingdom, from mammals to invertebrates[1]. Miple1 and Miple2 are homologues in *Drosophila*[100]. In the previous chapter, I described the expression patterns of *miple1* and *miple2* during *Drosophila* development. Among the tissues that express *miple2* are the embryonic mesoderm, the larval wing imaginal disc, and the adult testis. All three tissues are model systems in *Drosophila* developmental genetics for understanding mechanisms in signaling, branching morphogenesis, cell migration, and regulation of cell proliferation and differentiation.

The pattern of *miple2* expression in the embryonic mesoderm overlaps with that of *Drosophila* Anaplastic Lymphoma Kinase (Alk)[128]. Alk is a 180-kD protein that shares 34% identify and 48% similarity in amino acid sequence with ALK, a receptor tyrosine kinase and one of the putative Midkine and Pleiotrophin receptors identified in biochemical binding assays[25, 28, 43]. The phenotype of *alk*-null mutants has been well characterized. The visceral mesoderm-derived circular muscles that surround the gut fail to develop in *alk* mutants; consequently, *alk* mutants die during early larval

development[131]. Developmental, genetic, and biochemical studies confirm that the physiological ligand for Alk is Jelly belly (Jeb)[129, 130]. Jeb is a secreted protein with a type-A LDL receptor motif[132]. It bears no structural resemblance to Miple1, Miple2, Midkine, or Pleiotrophin. Together, Jeb-Alk signaling conveys positional information in specifying visceral muscle precursors during embryogenesis.

The unambiguous identification of Jeb as the ligand for Alk raises questions about the role of Midkine and Pleiotrophin as ligands for ALK. Whereas Jeb expression and its activation of Alk are limited to the mesoderm, Miple1 and Miple2 expression is ubiquitous[100, 128, 132]. Analyses of loss-of-function *alk* and *jeb* mutants suggest that Miple1 and Miple2 are insufficient to activate Alk. Other mechanisms are required to explain their action. They may be extracellular cofactors required for Jeb signaling. Alternatively, they may bind Alk as coligands.

My expression data suggest that in addition to the embryonic mesoderm, *miple2* is expressed in the larval wing imaginal disc, where three signaling pathways using the secreted molecules Hedgehog, Decapentaplegic (Dpp)/TGFβ, and Wingless/Wnt function to pattern the adult wing. Hedgehog and Dpp signaling pattern the wing along the anteroposterior axis, whereas Wingless signaling patterns the adult wing margin[133-135]. During embryogenesis, these same signals originating from the ectoderm subdivide the underlying mesoderm into Cartesian subdomains that give rise to distinct tissue lineages[136]. All three signaling pathways require heparan sulfate proteoglycans (HSPGs), which consist of a core protein to which heparan sulfate (HS) glycosaminoglycan (GAG) chains are attached. Biochemical binding assays have identified two HSPGs as putative receptors for Midkine and Pleiotrophin. They are N-syndecan, a transmembrane HSPG,

and Glypican-2, an extracellular HSPG tethered to the cell membrane via a glycosylphosphatidylinositol (GPI) anchor[61, 63, 64]. Syndecans and Glypicans are evolutionarily conserved molecules. In *Drosophila*, *sdc* encodes Syndecan, while *dally* and *dally-like protein* (*dlp*) encode two Glypican homologues[109-111].

Genetic and developmental data suggest that HSPGs are required in Wingless, Hedgehog, and Dpp signaling in the larval wing disc. Homozygous *dally* mutants phenocopy *wingless* and *dpp* mutants in wing patterning, and *dally* genetically interacts with components of both the Wingless and Dpp signaling pathways[110, 112, 116]. Dlp promotes Wingless activity in the wing at low levels of Wingless but opposes Wingless at high Wingless levels[113, 114]. Both *dally* and *dlp* mutants also phenocopy the wing patterning defects observed in *hedgehog* mutants; the phenotype is more severe in *dally, dlp* double mutants, implying functional redundancy between the two genes[115].

Since *miple2* expression and Wingless, Hedgehog, and Dpp signaling overlap in both the embryonic mesoderm and the larval wing disc, and Midkine and Pleiotrophin bind HSPGs *in vitro*, Miple2 may be a required cofactor in the Wingless, Hedgehog, and Dpp signaling pathways.

Whereas the development of the *Drosophila* embryonic mesoderm and the larval wing disc are established *in vivo* model systems for genetically dissecting the components of the signaling pathways, the *Drosophila* adult testis is an emerging system for studying the regulatory mechanism of cell proliferation and differentiation. During spermatogenesis, each germ line stem cell undergoes asymmetric division to give rise to a self-renewing daughter stem cell and a spermatogonial cell, which mitotically divides four more times before undergoing coordinated meiosis and differentiation that ultimately

gives rise to 64 mature sperms[137]. Genetic approaches have demonstrated that TGFβ signaling from the somatic cyst cell is required for the switch from mitotic proliferation to meiotic division in the undifferentiated spermatogonial cells, and EGFR signaling in the same cyst cells is required for the asymmetric cell division of the stem cells[138-140]. Since *miple2* is expressed in the testis, it may be a required cofactor in these signaling pathways.

In this study, I employed loss-of-function *Drosophila miple2* mutants to investigate the biological function of Midkine and Pleiotrophin. Visceral muscle development during embryogenesis is used as an *in vivo* assay to determine the requirement of Miple2 as a cofactor in Alk signaling. On the other hand, I used adult wing patterning as readout to investigate the potential role of Miple2 in Wingless/Wnt, Hedgehog, and TGFβ signaling in the larval imaginal disc. I also report here a male sterile phenotype potentially caused by the deletion of the *miple2* locus.

Materials and Methods

Southern blot genotyping

Genomic DNA was extracted from adult females in DNA extraction buffer (0.1 M NaCl, 0.2 M sucrose, 0.1 M Tris-HCl, pH 9.1, 50 mM EDTA, 0.5% SDS), precipitated with 95% ethanol, and resuspended in 0.1 M Tris-HCl pH 8.0. An equivalent of total DNA from 4 flies was used for overnight restriction endonuclease digestion at 37°C. Samples were resolved on 0.6% agarose gel, depurinated in 250 mM HCl, denatured in 0.5 M NaOH and 1.5 M NaCl, neutralized in 0.5 M Tris-HCl, 3 M NaCl, pH 8.0, and transferred to nitrocellulose membrane in 20x SSC overnight.

PCR-labeled digoxigenin probes (Roche) were used to detect the signals. The following primer pairs were used: *mipleI* left primer 5'-cagaagtcgcaccatgagaa-3', right primer 5'-cctttgcgagcagctttatc-3'; *mipleI* left primer 5'-ggctctgcacctagttttgg-3', right primer 5'- ccgtgttgttttcctccact-3'; *alk* left primer 5'-ctaatgatctcgcttgccgtgctcttc-3', right primer 5'- cactggtggttccaccttcgagttagg-3'. The following templates were used for the PCR reactions: ResGen clone RH72122 for *mipleI*; ResGen clone RE13914 *mipleI*; Tiling BAC clone BACR36P23 for *alk*. All clones were obtained from the Berkeley *Drosophila* Genome Project.

The digoxigenin labeled probes were used at 1:1000 dilution in DIG Easy Hyb buffer (Roche). Hybridization was carried out overnight at 37°C. Washes were carried out in 2x SSC, 0.1% SDS at room temperature, followed by 0.5x SSC, 0.1% SDS at 65°C. The membrane is then re-equilibrated in MAST solution (0.1 M maleic acid, 0.15 M NaCl, 0.3% Tween, pH 7.5), blocked with 1x dilution of blocking reagent (Roche) in MAST, and incubated with alkaline phosphatase conjugated anti-DIG antibody (Roche)

at 1:20,000 dilution in 1x blocking reagent in MAST at room temperature. The membrane was subsequently washed in MAST, equilibrated in detection buffer (0.1 M Tris-HCl, 0.1 M NaCl, pH 9.5). Signals were detected using CDP-Star reagent (Roche) and Kodak Biomax XAR film.

Membrane is stripped by washing in 0.2 M NaOH, 0.1% SDS at 37°C in two 15-minute washes, followed by rinsing in 2x SSC.

Fly genetics

The *piggyBac* alleles *miple1*^{c05178} and *miple2*^{c04774} were obtained from the Exelixis Collection maintained at Harvard University (stock numbers c05178 and c04774). The deficiency lines *Def(3L)BSC125* and *Def(3L)BSC126* are available from the Bloomington Stock Center (stock numbers 9290 and 9291). *miple2*-null flies were obtained by crossing the two deficiency lines. The temperature sensitive allele of *alk* was generated by the EMS mutagenesis screen carried out by the Charles Zuker laboratory and made available to the public at the *Drosophila* TILLING project at the University of Washington. The stock number for the temperature sensitive *alk* is *Z2-4587*. The PCR primers used to screen for the point mutation in *alk* are left primer 5'-ctaatgatctcgcttgccgtgctcttc-3', right primer 5'- cactggtggttccaccttcgagttagg-3'.

For the gentic interaction experiment, males heterozygous for the *miple* mutations on chromosome 3 placed over the *TM6b,Tb* balancer chromosome and crossed to *w; alk*^{ts}*/CyO; ftz,e/TM3,Sb* females. F1 males progeny with the genotype *w; +/CyO; miple/TM3,Sb* were selected for the presence of the dominant curly and stubble markers and crossed to virgin females with the genotype *alk*^{ts}*/alk*^{ts}*; ftz,e/TM3,Sb*. Males from the

F2 generation with the genotype *alk^{ts}/CyO; miple/TM3,Sb* were used for genetic interaction crosses to virgin females with the genotype *alk^{1}/CyO*.

The *UAS-miple1* and *UAS-miple2* transgenes were generated by directionally cloning the PCR products into the pUAST vectors[141]. The template sequences used for the transgenes are ResGen clone RH72122 for *miple1* and ResGen clone RE13914 for *miple2*. The PCR primers were designed such that the the recognition sequences for Not I and Xho I restriction endonucleases are linked to the left and right primers, respectively, to enable the directional cloning of the PCR product into the pUAST vector. In addition, DNA sequence encoding the hemagluttin (HA) epitope tag was attached to the right primer such that the transgenes will express HA-tagged Miple1 and Miple2 proteins. Actual primer sequences used for are *miple1* left primer 5'-gcggccgcatgagaattaattgcaacgc-3', *miple1* right primer 5'-ctcgagttaagcgtagtctgggacgtcgtatgggtaaacgcgtcctttgcgagcag -3', *miple2* left primer 5'-gcggccgcatgaatcttatactggcttt -3', *miple2* right primer 5'-ctcgagtcaagcgtagtctgggacgtcgtatgggtaagacgaaatgtgactgg -3'. Transgenic flies were generated by the injection of pUAST constructs at Model Systems Genomic at Duke University. Injected female flies were crossed to *yw* males, and transgenic flies were recovered in the F1 generation based on the presence of the mini-*white* marker on the pUAST vector.

All crosses are carried out at room temperature unless specified.

RT-PCR

RT-PCR was performed as described in the previous chapter.

Western blot analysis

Protein from 10 homogenized adult fly heads was isolated in PBS and Lammeli buffer. An equivalent of total protein from one fly head is loaded per lane. Proteins are resolved on a 15% SDS-PAGE acrylamide gel. Rabbit anti-Miple1 antiserum was used at 1:1000 dilution.

Immunohistochemistry

Immunohistochemical techniques were used as described in the previous chapter. The blocking step for anti-MHC immunostaining used PBT with 0.3% Triton X-100 and 0.3% BSA. All primary antibody incubations were carried out overnight at 4°C in PBTA. Antibody dilution factors are as follows: rabbit anti-MHC 1:500; rabbit anti-βgal 1:500.

Testes squash and DAPI staining

Testes from 5-day old males were dissected out in testes buffer (15mM KH_2PO4, 80 mM KCl, 16 mM NaCl, 5 mM $MgCl_2$, 1% polyethylene glycol), placed on poly-L-lysine coated slides, squashed with cover glass and frozen in liquid nitrogen. The cover glass is subsequently removed using a razor blade, and the slide was placed in 95% ethanol on dry ice for 10 minutes. The slides were then drained and the testes were fixed with 4% formaldehyde (Polysciences) in PBS for 7 minutes at room temperature, followed by two 15-minute washes in testes wash buffer (PBS with 0.3% Triton-X100, 0.3% sodium deoxycholate). The testes were then rinsed in PBS, and blocked with blocking solution (PBS with 0.1% Triton-X100, 3% BSA) for 30 minutes. DAPI stain was performed using 1 μg/ml DAPI in blocking solution, followed by two 10-minute

washes in blocking solution. The samples were subsequently mounted in Slow Fade Gold (Invitrogen) mounting medium for fluorescence microscopy.

For phenotypic analysis of testes and sperm morphology, the entire male reproductive tract was dissected from freshly eclosed males in Hoyle's medium. Tungsten needle was used to puncture the seminal vesicles. The samples were mounted on slides in PBS, covered with a cover slip, and photographed using phase contrast microscopy using Zeiss Axioskop 2.

Results

Genotyping and characterization of *mipIe2* mutants

A *mipIe2*-null mutant was generated by crossing two overlapping deficiencies, *Def(3L)BSC125* (*BSC125*), and *Def(3L)BSC126* (*BSC126*). The *BSC125* deficiency harbors a 10.2-kb deletion that brackets both *mipIe1* and *mipIe2* loci; *BSC126* contains a 56-kb deletion that selectively removes *mipIe2*[104]. Each deficiency is homozygous lethal. The region of overlap between the two deficiencies covers two additional genes that have not been characterized to date. They are *cg32845*, located in intron 1 of the *mipIe2* loci, and *cg12313*, which lies downstream of *mipIe2* (Figure 3.1A). Southern blot genotyping confirms the deletion of *mipIe2* in flies *trans*-heterozygous for the two deletions (Figure 3.1B, C). Females carrying both deficiencies in *trans* are viable and fertile. Males of the same genotype are viable but sterile.

In addition to the *mipIe2*-null *trans*-heterozygous flies, I obtained a novel *mipIe2* allele, *mipIe2*^{c04774}, generated in a genome wide gene disruption project using the *piggyBac* transposable element[105]. Mapping by inverse PCR suggests that the *piggyBac* insertion site is located in the first intron of the *mipIe2* gene (Figure 2D). I genotyped the flies using Southern blot analysis in order to independently verify the inverse PCR findings. My findings are consistent with the inverse PCR data (Figure 2F). In addition, I discovered a second insertion site located between the Nhe I and Spe I restriction endonuclease sites located in exon 5 of the *mipIe1* loci and downstream of the *mipIe1* coding region. This second insertion most likely results from a local hop of the *piggyBac* transposable element. Flies homozygous for the *mipIe2*^{c04774} allele are viable and fertile.

I also investigated *mipIe2* mRNA expression in the *mipIe2* mutant by performing RT-PCR on total RNA isolated from ovaries, which normally express the *mipIe2* message. I detected no *mipIe2* message in *BSC125/BSC126* ovaries, while females homozygous for *mipIe2*^{c04774} express significantly reduced levels of *mipIe2* compared to wild type and heterozygous controls (Figure 2.7E).

Genotyping and characterization of *mipIe1* mutant

I obtained a *mipIe1* allele, *mipIe1*^{c05178}, generated in the *piggyBac* gene disruption project (Harvard collection stock number c05178)[105]. Inverse PCR maps the site of *piggyBac* insertion to exon 1 of the *mipIe1* gene (Figure 3.2A). My southern genotyping results are consistent with the inverse PCR findings (Figure 3.2B, C).

I analyzed *mipIe1* gene expression at the levels of mRNA and protein expression. RT-PCR using total RNA isolated from the adult head revealed that the combination of *mipIe1*^{c05178} in *trans* with the *mipIe1, mipIe2* double mutant *BSC125* deficiency results in significantly decreased levels of *mipIe1* message (Figure 3.2D). However, Western blot analysis using rabbit anti-Miple1 antiserum revealed that Miple1 protein is present in the adult head of flies homozygous for the *mipIe1*^{c05178} allele, and in the heads of the *trans*-heterozygous *mipIe1*^{c05178}*/BSC125* adults (Figure 3.2E).

Homozygous *mipIe1*^{c05178} flies are viable and fertile, as are *mipIe1*^{c05178}*/BSC125* *trans*-heterozygous mutants.

Genotyping and characterization of *mipple1, mipple2* double mutant

The *Def(3L)BSC125* line harbors a 10.2-kilobase deletion in the 61B3 cytological region on chromosome 3L (Figure 3.1A). The deletion removes both the *mipple1* and *mipple2* loci[104]. In addition, it brackets the essential *mRpL17* gene, which encodes a component of the mitochondrial ribosome large subunit. Additional genes deleted in this deficiency include the yet uncharacterized genes *cg13879, cg12313, cg32845,* and *Tudor-SN.* Moreover, the expression of *dip2*, located in the region flanking the deficiency, may be affected, since the progenitor line used to generate the *BSC125* deficiency carries a *piggyBac* transposable element inserted into the 5' cis regulatory region of *dip2*.

Approximately 60% of the homozygous *BSC125* embryos hatch as larvae, compared to 96% of wild type control and 86% of embryos homozygous for a P-element insertion into the 5' cis regulatory region of the essential *mRpL17* gene. Homozygous mutant larvae of both genotypes die within the first 72 hours after hatching. Genotyping by Southern blot analysis confirms the deletion of both *mipple1* and *mipple2* loci in the homozygous larvae (Figure 3.3B-D).

Analysis of *mipple1* and *mipple2* mutants with respect to Alk signaling

I analyzed single mutants in *mipple1* and *mipple2*, as well as the *mipple1, mipple2* double mutant deficiency *BSC125* with respect to Alk signaling. Since our expression data suggested that maternal *mipple1* and *mipple2* are present in the embryos prior to the onset of zygotic transcription, I reduced or removed maternal *mipple1* and *mipple2* contribution, respectively. *mipple1* mutant embryos were generated by crossing males heterozygous for *BSC125* to *mipple1*^{c05178}*/BSC125 trans*-heterozygous *mipple1* mutant

females. *mipple2*-null embryos were generated by crossing *BSC125* heterozygous males to *mipple2*-null, *BSC125/BSC126 trans*-heterozygous females. Mutant *mipple1* or *mipple2* offspring in each cross reached adult stage at expected Mendelian ratios. Immunostaining the embryos with rabbit anti-myosin heavy chain (MHC) revealed no disruption in visceral muscle formation (Figure 3.4A-C).

I attempted to remove maternal contribution of both *mipple1* and *mipple2* by somatic recombination in the germline cells of females heterozygous for the *BSC125* deficiency. However, these females are sterile. Consequently, I was unable to analyze the phenotype of *mipple1, mipple2* double mutants in the absence of maternal contribution. Homozygous embryos born to heterozygous *BSC125* parents demonstrated midgut development pattern indistinguishable from that of wild type based on anti-MHC immunostaining (Figure 3.4D, E).

Since phenotypic analysis failed to provide conclusive developmental evidence for the requirement of *mipple1* and *mipple2* in Alk function during embryogenesis, I employed a genetic approach to investigate the potential role of *mipple1* and *mipple2* in Alk signaling. I have identified a novel allele of *alk* using PCR-based TILLING (Targeting Induced Local Lesions in Genomes) screening of a collection of EMS-mutagenized lines generated in the laboratory of Charles Zuker[103]. This novel allele, $alk^{Z2\text{-}4587}$ (Seattle TILLING Project Stock number Z2-4587), carries a missense mutation that results in the replacement of the evolutionarily conserved asparagine 1255 within the tyrosine kinase domain with aspartate.

When placed in *trans* with the null alk^{1} allele, $alk^{Z2\text{-}4587}/alk^{1}$ *trans*-heterozygous flies are viable at 18°C and lethal at 29°C (Figure 3.5D)[131]. At the intermediate

temperature of 22°C, 78% of the *trans*-heterozygotes in the F1 generation eclose as adults. Anti-myosin staining of embryos collected at 29°C revealed identical disruptions in midgut musculature in homozygous alk^{1}/alk^{1} and *trans*-heterozygous $alk^{Z2\text{-}4587}/alk^{1}$ embryos, demonstrating that the novel allele behaves as a null allele at nonpermissive temperatures (Figure 3.5A-C). Results from my temperature shift experiments, in which I moved the *trans*-heterozygous mutants from 18°C to 29°C at various time points during development, suggest that the critical period for the lethal phenotype in *alk* mutants takes place during embryogenesis, within 24 hours after egg laying.

The partial lethal phenotype of the $alk^{Z2\text{-}4587}$ allele in combination with alk^{1} at intermediate temperatures provides a sensitive assay with which I was able to determine the requirement for Miple1 and Miple2 as cofactors in Alk signaling. I investigated the role of *miple1* and *miple2* as dominant modifiers of *alk* by comparing the viability of the alk^{ts}/alk^{1} *trans*-heterozygous mutant adults in the sensitized *miple1* and *miple2* mutant backgrounds with the viability of the *trans*-heterozygous mutants in the control wild type genetic background. The scheme of the crosses is outlined in Figure 3.6A. I used three different sensitized genetic backgrounds: the *BSC125* deficiency as the *miple1, miple2* double mutant, and the *piggyBac* alleles $miple1^{c05178}$ and $miple2^{c4774}$ as single mutants. The $miple2^{c04774}$ *piggyBac* allele was chosen over the *miple2*-null *BSC126* deficiency line because the deletion in the deficiency line brackets a loci encoding a Rho GTP exchange factor, which functions downstream of receptor tyrosine kinase signaling[142]. Compared to wild type genetic background control siblings produced in the same cross, I observed differences in alk^{ts}/alk^{1} *trans*-heterozygote viability of no greater that 10% in each of the

three modifier backgrounds (Figure 3.6B). I interpreted these results as *mipple1* and *mipple2* do not behave as dominant modifiers of Alk signaling during embryogenesis.

mipple2 and patterning in the adult wing

I investigated the requirement for Mipple2 as a cofactor in HSPG-dependent Wingless, Hedgehog, and Decapentaplegic signaling pathways, which function during larval development to pattern the adult wing, using flies lacking both maternal and zygotic *mipple2*. Compared to wild type adult wings, *mipple2*-mutant wings are indistinguishable in patterning along the anteroposteior axis and at the wing margin (Figure 3.7A, B). Overexpression of either the *UAS-mipple1* or *UAS-mipple2* transgene using the wing imaginal disc specific *1096gal4* driver line also produced adult flies with wing patterning indinstinguishable from that found in wild type adults (Figure 3.7C, D).

Defective spermatogenesis in *mipple2*-null, *Def(3L)BSC125/Def(3L)BSC126* males

The *mipple2*-null *BSC125/ BSC126* flies cannot be propagated in the absence of a balancer chromosome. Outcrossing males and females mutants to wild type flies revealed that males *trans*-heterozygous for the deficiencies are sterile. The phenotype has 100% penetrance based on results from multiple crosses.

Examination of contents released from ruptured seminal vesicles demonstrated defective sperm production in *trans*-heterozygous flies. The phenotype varies from bundled, nonmotile sperm to debris-filled seminal vesicles completely devoid of sperm (Figure 3.8A-C). DAPI staining of testes revealed indistinguishable patterns of nuclei staining at the apex in both *trans*-heterozygous mutants and control siblings carrying a

balancer chromosome wild type for *miple2, cg32845* and *cg12313* (Figure 3.8D, E). These findings suggest that *miple2* and the two additional genes covered in the overlap are not required for the maintenance of the stem cells in the testis. Live testes squashes observed under phase contrast microscopy revealed the presence of 64-spermatid stage cysts that represent the penultimate stage in spermatogenesis in both the *trans*-heterozygous mutants and control siblings (Figure 3.8F, G). Taken together, our findings indicate that the *BSC125/BSC126 trans*-heterozygotes are defective in spermatid individualization. Previously published results classify these mutants as having the "classical" male sterile phenotype[143].

Discussion

miple1, miple2 and Anaplastic Lymphoma Kinase signaling

Developmental data produced in this study do not provide conclusive evidence that *miple1* and *miple2* are required cofactors in Alk signaling. The absence of a lethal phenotype in mutants lacking both maternal and zygotic *miple2* suggests possible functional redundancy between *miple1* and *miple2.* This theory is consistent with my expression data, which indicates overlapping patterns of expression of both genes in multiple tissues during various stages of development. Removal of both *miple1* and *miple2* from the maternal germ line in the absence of zygotic rescue would be the best approach to generate conclusive developmental data for the requirement of Miple1 and Miple2 in Alk signaling. However, since mosaic females homozygous for the *miple1, miple2* double-mutant *BSC125* deficiency in the germline are sterile, I was unable to use phenotypic correlation to establish a requirement for Miple1 and Miple2 in Alk signaling.

On the other hand, my genetic interaction studies using the temperature sensitive $alk^{Z2\text{-}4587}$ allele in the *miple1* and *miple2* mutant backgrounds suggest that Miple1 and Miple2 are not involved in Alk signaling. I scored for partial lethality of the $alk^{Z2\text{-}4587}$ allele in combination with the null alk^{1} allele at intermediate temperatures. Previous studies have demonstrated that the lethal phenotype in *alk* mutants is caused by defects in visceral mesoderm development during embryogenesis[131]. I confirmed these findings by demonstrating in our temperature shift experiments that our alk^{ts}/alk^{1} *trans*-heterozygous mutants survive to adulthood if they are kept at permissive temperatures for the first 24 hours after egg laying, a period that corresponds to embryogenesis. Using embryonic

visceral mesoderm development as readout, my genetic interaction data do not establish a direct link between Miple1, Miple2 and Alk signaling.

My findings are consistent with recently published Pleiotrophin-Alk interaction data based on tissue culture studies. Previously, it was demonstrated that the addition of Pleiotrophin or Midkine to 293T cells transiently expressing Alk lead to the activation of MAP kinase and PI3 kinase signaling cascades downstream of Alk. However, 293T cells constitutively express RPTPβ/PTPζ, a putative Pleiotrophin and Midkine receptor identified in biochemical binding assays. The latest studies employed MCF-7 or SH-SY5Y cells, which do not express RPTPβ/PTPζ. Pleiotrophin failed to activate Alk in both studies[144, 145]. These results led to an alternative model for Alk activation: Midkine and Pleiotrophin bind RPTPβ/PTPζ as inhibitory ligands that inactivate phosphatase activity. The accumulation of phosphorylated Alk and the activation its downstream MAP kinase and PI3 kinase signaling pathways are indirect effects secondary to phosphatase inactivation.

The latest tissue culture findings on the mechanism of Alk activation present a potential confounding factor to the interpretation of *alk-miple1, miple2* genetic interaction results. Expression data available at the Berkeley *Drosophila* Genome Project (BDGP) website suggests that Ptp4E, a *Drosophila* receptor protein tyrosine phosphatase, is expressed in the endoderm and the mesoderm during embryogenesis. The timing of *ptp4E* expression overlaps with that of *miple2*. To date, *ptp4E* mutants have not been characterized. A potential function of Ptp4E, which is structurally and catalytically homologous to RPTPβ/PTPζ, is to modulate the MAP kinase and PI3 kinase signaling cascades downstream of the receptor tyrosine kinases in the embryonic endoderm and

mesoderm. It is possible that Ptp4E, which is also expressed in the embryonic CNS, is the biological receptor for both Miple1 and Miple2. Taking Ptp4E into consideration, any modification of the partial lethal phenotype in $alk^{Z2\text{-}4587}/alk^{1}$ *trans*-heterozygous mutants by *miple1* or *miple2* still would not provide conclusive evidence establishing Miple1 and Miple2 as cofactors or alternative ligands in Alk activation. The absence of interaction between *miple1* and *miple2* with *alk*, on the other hand, points to the likelihood that Alk, Miple1 and Miple2 act in non-overlapping and functionally distinct signaling pathways, despite their overlapping patterns of expression in the mesoderm and the CNS.

Miple2 and adult wing patterning

Phenotypic analysis in adult wing patterning using *miple2*-null flies demonstrated no gross disruption in patterning. The most likely explanation is the functional redundancy between Miple1 and Miple2. Although I have not detected higher-than-background levels of *miple1* mRNA expression in the wild type imaginal discs, I have not examined *miple1* expression in the imaginal discs of *miple2*-null flies. On the other hand, transgenic flies overexpressing *miple1* or *miple2* in the wing disc also do not exhibit a patterning defect. These findings suggest that Miple1 and Miple2 are not sufficient to alter Wingless/Wnt, Hedgehog, or Dpp/TGFβ signaling in the larval wing disc.

Although our *miple2* mutant flies and transgenic flies overexpressing *miple1* and *miple2* failed to produce phenotypic data suggesting the requirement for Miple2 in morphogen signaling in the wing disc, evidences presented in this study do not exclude the possibility that both Miple1 and Miple2 function as cofactors in morphogen signaling.

Alternative techniques could be employed in the future to investigate in detail the roles of Miple1 and Miple2 in Wingless/Wnt, Hedgehog, Dpp/TGFβ, and FGF signaling. One method remains the genetic interaction approach. The *miple1, miple2* double mutant *BSC125* deficiency could be introduced into sensitized genetic backgrounds in combination with hypomorphic alleles of genes encoding components of the Wingless, Hedgehog, Decapentaplegic/TFGβ, and FGF signaling pathways. Alternatively, somatic recombination could be used to generate clones of cells homozygous null for *miple1* and *miple2*. However, there remains the possibility that maternal contribution of *miple1* and *miple2* could continue to mask any potential loss-of-function phenotype in the clones.

Male sterile phenotype in *miple2*-null *BSC125/BSC126* mutants

A potential phenotype in our *miple2*-null mutants is male sterility. However, the region of overlap covered by the parental deficiency lines also includes two yet uncharacterized genes: *cg32845* and *cg12313*. Further analyses of the male sterile phenotype must be preceded by the demonstration that the male sterile phenotype is specific for the deletion of *miple2*.

Two approaches can be used to directly address the *miple2* specificity for the male sterile phenotype seen in the *BSC125/BSC126 trans*-heterozygous mutants. One would be the isolation of a null *miple2* allele. However, such attempts are complicated by the fact that *miple2* is a nonessential gene, which increases the difficulty for the recovery of null alleles of *miple2* generated in any targeted mutagenesis attempt. One way to bypass this potential obstacle would be the PCR-based TILLING screening for single nucleotide polymorphisms induced by EMS mutagenesis. Indeed, the laboratory of

Charles Zuker maintains a large collection of EMS mutagenized, nonlethal lines that is available to the *Drosophila* research community[103]. Since a large number of alleles generated in EMS mutagenesis contain nonsense mutations, there is likelihood that a null *miple2* allele will be recovered. Alternatively, Flp-mediated recombination between two FRT-containing *piggyBac* elements in *trans*, with each element inserted in a different location within the *miple2* loci, can be employed to generate micro deletions in the *miple2* loci such that a functional *miple2* protein cannot be produced[104].

The second approach to demonstrate that the loss of the *miple2* loci causes the male sterile phenotype would be the transgene rescue experiment. The restoration of fertility in males expressing the *UAS-miple2* transgene in the testis would be sufficient to demonstrate the specific requirement for *miple2* in spermatogenesis.

Spermatogenesis in *Drosophila* has been used as a model system to understand signaling in stem cell maintenance. Three populations of cells are found at the apex of the *Drosophila* testis: hub cells that form the stroma of the testis, and two populations of stem cells, the somatic cyst cells and the germline gonial cells. In the larval and adult testes, hub cells express the *hedgehog* gene, while TGFβ signaling in the cyst cells is responsible for the germline cells to switch from mitosis to meiosis during sperm differentiation[137, 139]. My expression data suggest that the *miple2* message is present during early stages of spermatogenesis. Miple2 may have a potential role in facilitating Hedgehog and TGFβ signaling in the context of stem cell maintenance and meiosis regulation. However, morphological analyses of *BSC125/BSC126 trans*-deficient mutants reveal a normal pattern of nuclear staining at the apical tip of the testis indicative of a functional germ cell stem cell niche. Examination of latter stages of spermatogenesis

demonstrated the presence of meiotic cells, and the 64-spermatozoa cysts in the mutant testes. These findings suggest that *miple2* alone is not necessary for these steps. Given the overlapping patterns of *miple1* and *miple2* expression throughout development, Miple1 and Miple2 may have redundant functions in Hedgehog and TGFβ signaling in the testis.

The *BSC125/BSC126 trans*-deficient males exhibit the so-called "classic" male sterile phenotype. In this class of mutants, spermatogenesis arrests at the penultimate 64-spermatid cyst stage and fails to proceed to the final individualization step. The classic male sterile phenotype is reported in 68% of total male sterile mutants recovered in previous genetic screens. While to date the exact number of complementation groups have not been determined, analyses of selected mutants belonging to this phenotypic class revealed that disruption in genes required in earlier stages of spermatogenesis may result in the arrest of sperm development at the sperm individualization step. One hypothesis is that the individualization step serves as a final checkpoint to eliminate any abnormalities from the sperm pool[143].

While the significant number of uncharacterized "classic" male sterile phenotypes makes a direct correlation between the potential *miple2*-null male sterile phenotype and Miple2 protein function difficult, a reasonable model can be constructed based on available data from Midkine and Pleiotrophin tissue culture experiments and the expression patterns of *miple1* and *miple2* as determined in my expression analyses. The process of spermatid individualization requires the formation of the individualization complex (IC), a structure consisting of cytoskeletal proteins and the cell membrane[146]. The IC forms near the head of the spermatozoa, which is localized near the base of the testis. It migrates down the length of the spermatozoa toward the apex. As the complex

migrates apically, it separates the individual spermatids into 64 individual sperm cells. The assembly and subsequent migration of the individualization complex may require extracellular signals, which may in turn require Mple2 function. Indeed, tissue culture experiments have repeatedly demonstrated that both Midkine and Pleiotrophin are capable of promoting neurite outgrowth and branching morphogenesis that involve the assembly and rearrangement of cytoskeletal components. My expression data on *mple1* and *mple2* during embryogenesis have also demonstrated that both genes are expressed in cells undergoing cell shape change: the migrating cells of the embryonic endoderm and mesoderm express *mple2*, while Mple1 protein localizes to the glial processes ensheathing the axon tracts.

Although the specificity of *mple2* mutation in causing the classic male sterile phenotype in the *BSC125/BSC126 trans*-heterozygous mutants remains to be determined, it is nevertheless interesting that *mple2* expression is found in the testis. The presence of *mple2* mRNA implies a potential requirement for Mple2 function during spermatogenesis, and the expression of *mple2* during spermatogenesis is correlated with spermatozoa maturation, a step itself involves cell elongation secondary to cytoskeletal reorganization.

Based on observations in the testis, the expression data of *mple1* and *mple2* throughout development, and tissue culture results published previously, Mple1 and Mple2 likely function in signaling pathways that result in cytoskeletal changes. Therefore, future investigations into Mple1 and Mple2 function in *Drosophila* that focus on signaling pathways that elicit cytoskeletal rearrangement in target cells are most likely to uncover the biological roles of Midkine and Pleiotrophin.

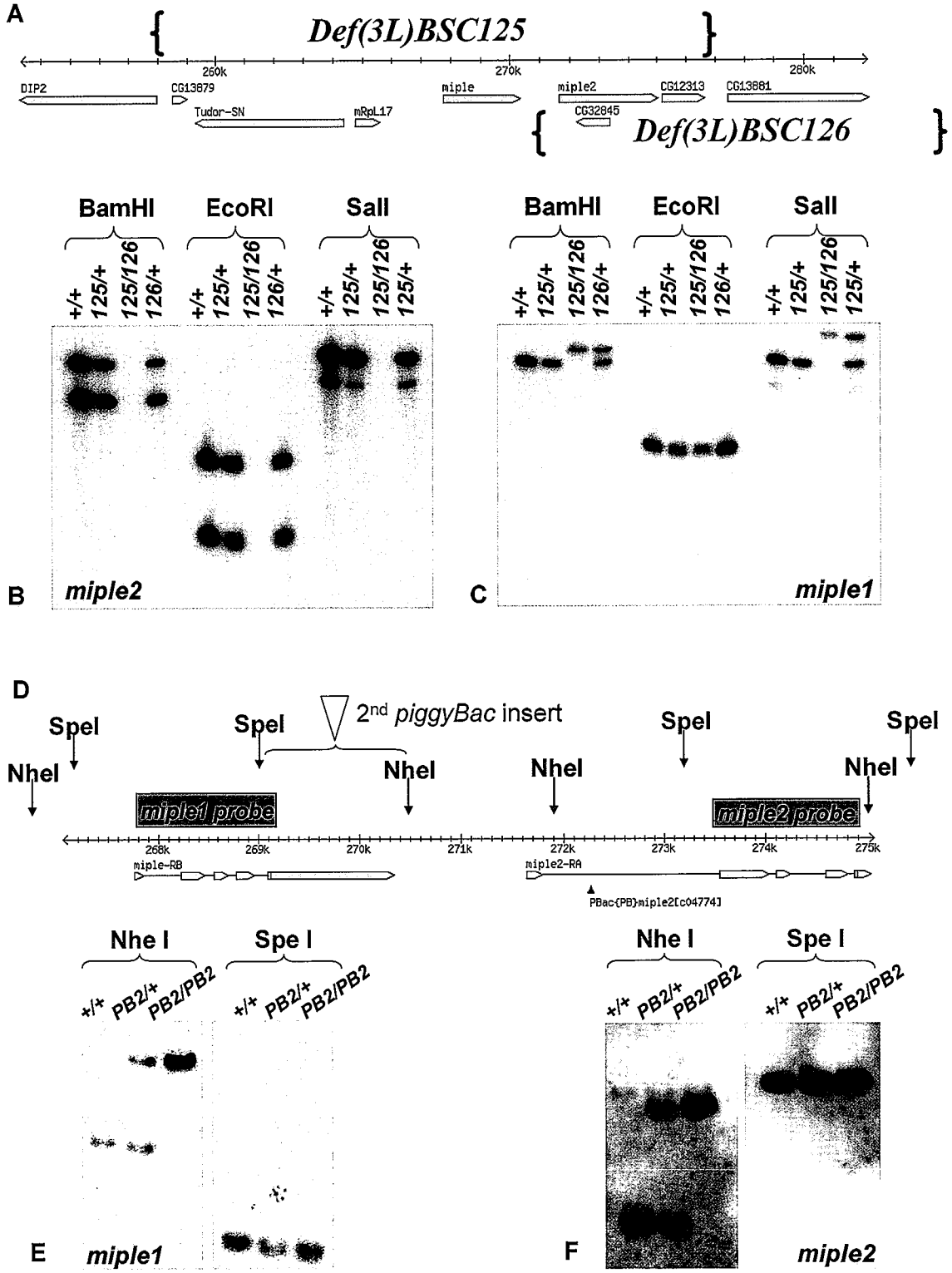
A
Def(3L)BSC125
260k
270k
280k
DIP2
CG13879
Tudor-SN
mRpL17
miple
miple2
CG32845
CG12313
CG13881
Def(3L)BSC126
BamHI
EcoRI
SalI
+/+
125/+
125/126
126/+
125/+
125/126
125/+
B
miple2
BamHI
EcoRI
SalI
+/+
125/+
125/126
126/+
125/+
125/126
126/+
C
miple1
D
SpeI
SpeI
2nd piggyBac insert
SpeI
SpeI
NheI
NheI
NheI
NheI
miple1 probe
miple2 probe
268k
269k
270k
271k
272k
273k
274k
275k
miple-RB
miple2-RA
PBac{PB}miple2[c04774]
Nhe I
Spe I
+/+
PB2/+
PB2/PB2
+/+
PB2/+
PB2/PB2
E
miple1
Nhe I
Spe I
+/+
PB2/+
PB2/PB2
+/+
PB2/+
PB2/PB2
F
miple2

Figure 3.1. Genotyping of *miple2* mutants.
(A) Schematic of the genomic region in the vicinity of the *miple1* and *miple2* loci on chromosome 3L. Genes spans are depicted in blue. Brackets indicate the regions of deletion covered by the parental Exelixis deficiency lines *Def(3L)BSC125* (green) and *Def(3L)BSC126* (red) used to generate the *miple2*-null fly.
(B and C) Southern blot genotyping of the *miple2*-null fly. DNA samples are isolated from wild type flies (+/+), flies heterozygous for parental deficiencies *BSC125* (*125/+*) and *BSC126* (*126/+*), and *miple2*-null *BSC125/BSC126* adult flies. *miple2*-probed blot shows the absence of a signal in *BSC125/BSC126* lane (B), while *miple1*-probed blot detects the presence of a fragment identical to that seen in the *BSC126/+* lane (C).
(D) Schematic depiction of genomic region in the vicinity of the *miple1* and *miple2* loci in *piggyBac* allele *miple2c*^{04774}. The schematic includes the relative positions of the *miple1* and *miple* loci, with the exons depicted as block arrows and coding regions in orange. The genomic region recognized by the probe is labeled in pink. Also pictured are the published *piggyBac* element insertion site as determined by inverse PCR (blue triangle labeled PBac{PB}miple2[c04774]), a potential second insertion site produced in a local hop, and the Nhe I and Spe I restriction endonuclease sites used for insertion mapping.
(E and F) Southern blot membrane with genomic DNA digests of wild type flies (+/+), flies heterozygous (*PB2/+*) and homozygous (*PB2/PB2*) for the *miple2c*^{04774} allele probed with *miple2* (E) and *miple1* (F) probes.

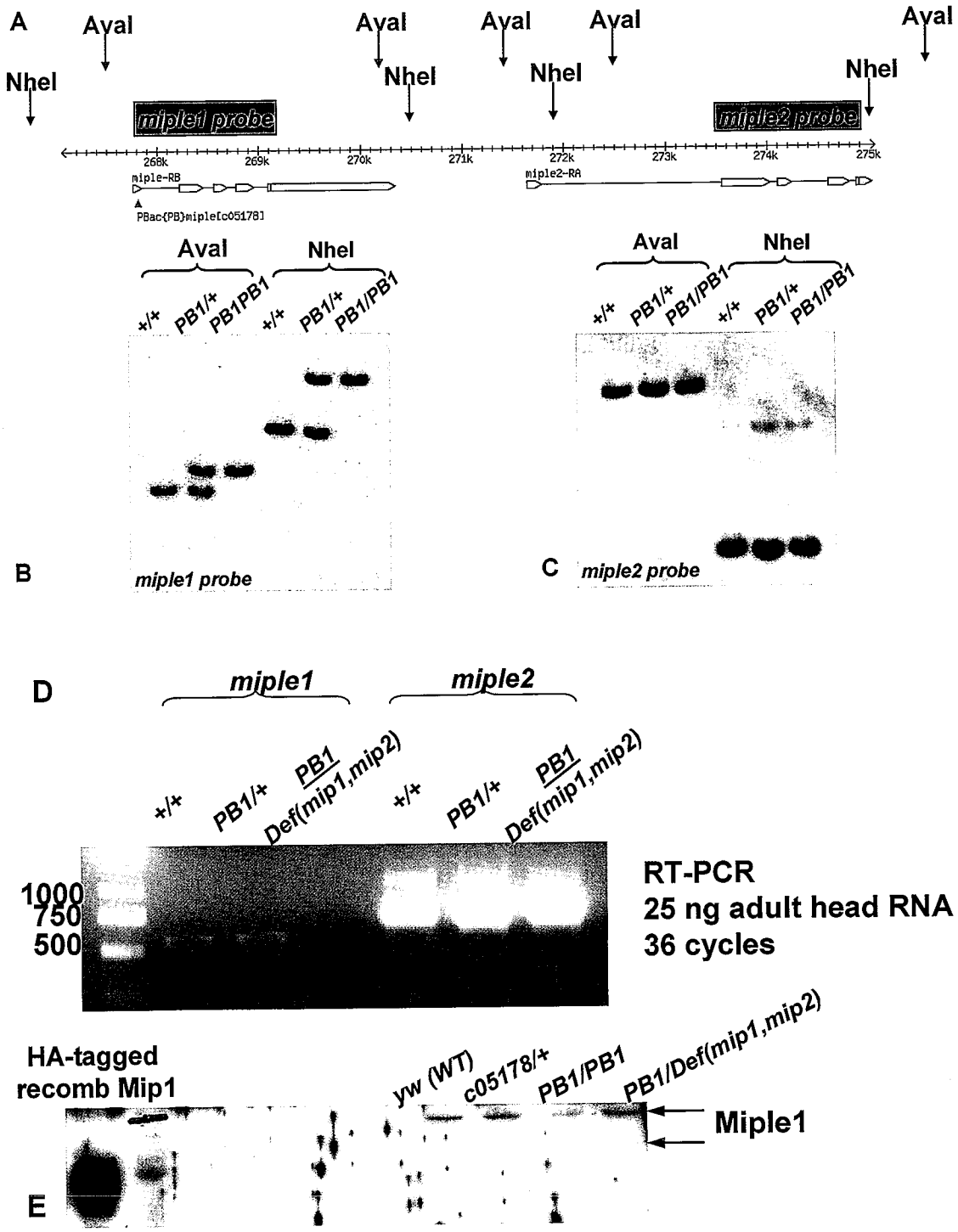

Figure 3.2. Genotyping and characterization of *piggyBac-mipIe1* allele.
(A) Schematic depiction of the genomic region in the vicinity of the *mipIe1* and *mipIe2* loci in *piggyBac* allele *mipIe1*^{c05178}. The schematic includes the relative positions of the *mipIe1* and *mipIe2* loci. Exons are depicted as block arrows, and coding regions are colored orange. The genomic region recognized by the probe is labeled in pink. Also

pictured are the published *piggyBac* element insertion site as determined by inverse PCR (blue triangle labeled PBac{PB}miple [c05178]), and the Nhe I and Ava I restriction endonuclease sites used for insertion mapping.
(B) *miple1*- and (C) *miple2*-probed Southern blot membranes with genomic DNA isolated from wild type (+/+) flies and flies heterozygous (*PB1/+*) and homozygous (*PB1/PB1*) for the $miple1^{c05178}$.
(D) RT-PCR of total RNA isolated from adult heads with wild type (+/+), heterozygous $miple1^{c05178}$ (*PB1/+*), and $miple1^{c05178}$/ *BSC125* (*PB1/Def(mip1, mip2)*) genotypes. 25 ng of total RNA was amplified for 36 cycles for both *miple1* and *miple2* (control). Reduced *miple2* message is detected in *piggyBac-miple1/ BSC125* adults.
(E) Western blot analysis of total protein extracted from adult head of wild type flies (*WT*), flies heterozygous (*PB1/+*), and homozygous (*PB1/PB1*) for the $miple1^{c05178}$ allele, and $miple1^{c05178}$/ *BSC125* (*PB1/Def(mip1,mip2)*) transheterozyotes. HA-tagged recombinant Miple1 is used as a positive control. Miple1 is detected as a doublet in all four genotypes.

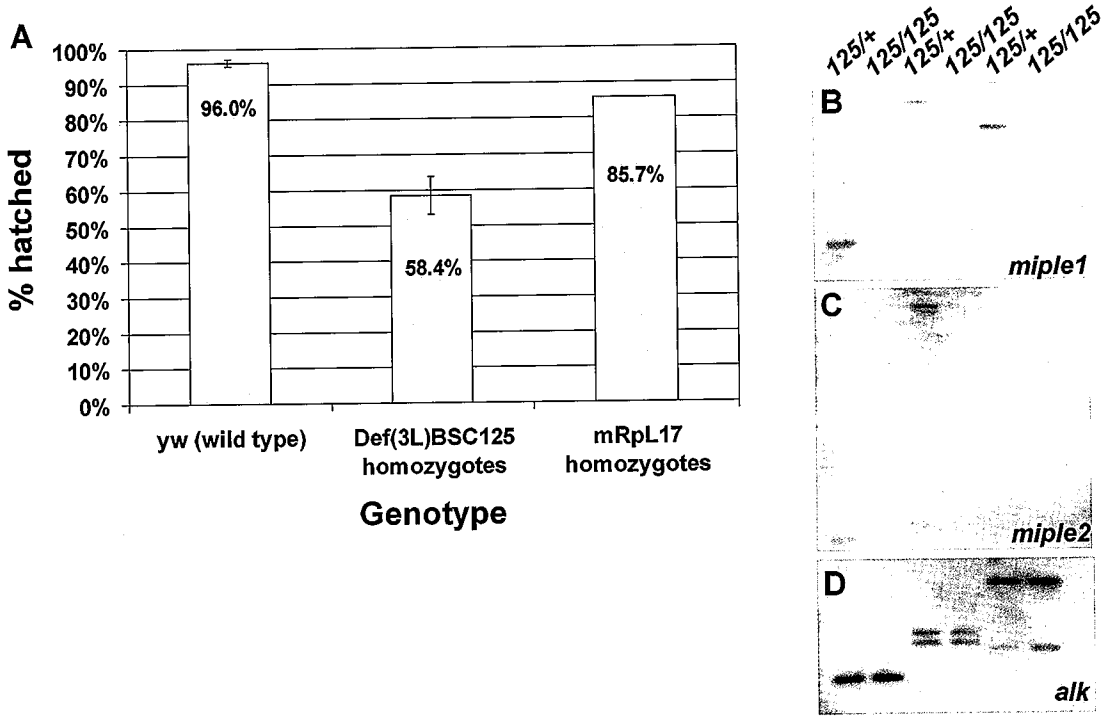

Figure 3.3. Characterization of *miple1, miple2* double mutant *Def(3L)BSC125.*
(A) Bar graph demonstrating the percent of wild type embryos, embryos homozygous for the *BSC125* deficiency, and embryos homozygous for the P element insertion in *mRpL17* that hatch as 1st instar larvae.
(B-D) Southern genotyping of *BSC125* mutants. Restriction digest of genomic DNA isolated from 1st instar larvae homozygous (*125/125*) and heterozygous (*125/+*) for the deficiency hybridized with DNA probes with sequences corresponding to (B) *miple1*, (C) *miple2*, and (D) *alk*. Signals corresponding to restriction fragments containing *miple1* and *miple2* are absent in lanes loaded with DNA isolated from larvae homozygous for the *BSC125* deficiency.

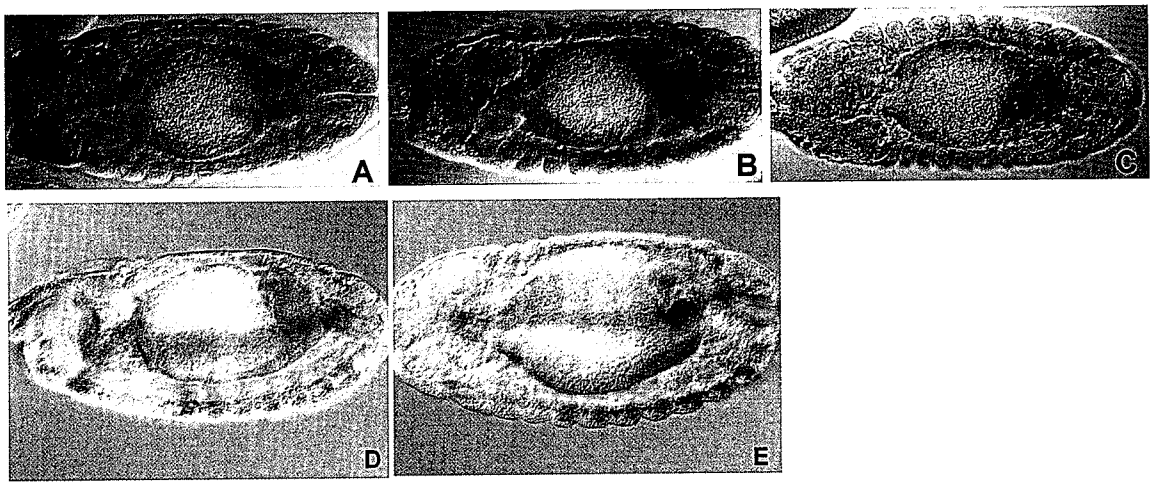

Figure 3.4. Single *miple1, miple2* mutants and *miple1, miple2* homozygous offspring born to parents heterozygous for *Def(3L)BSC125* deficiency have normal gut structure.

(A-C) Overhead views of whole mount stage 15 embryos immunostained with anti-myosin heavy chain (MHC) and anti-βgal antisera followed by DAB reaction. Anterior is to the left for all panels.

(A) Control embryo heterozygous for the *Def(3L)BSC125* deficiency.

(B) *miple1* mutant embryos produced by crossing heterozygous *BSC125* males to *miple1*^{c05178}*/BSC125 miple1* mutant females.

(C) *miple2*-null embryos produced by crossing heterozygous *BSC125* males to *miple2*-null *BSC125/BSC126* females. Embryos in all three classes show positive immunoreactivity against MHC in tissues lining the midgut, and the proper containment of the yolk content within the constricting midgut.

(E-F) Lateral views of whole mount stage 15 embryos immunostained with rabbit anti-MHC antisera. MHC immunostaining is observed in both wild type (D) and homozygous *BSC125* born to heterozygous parents (E).

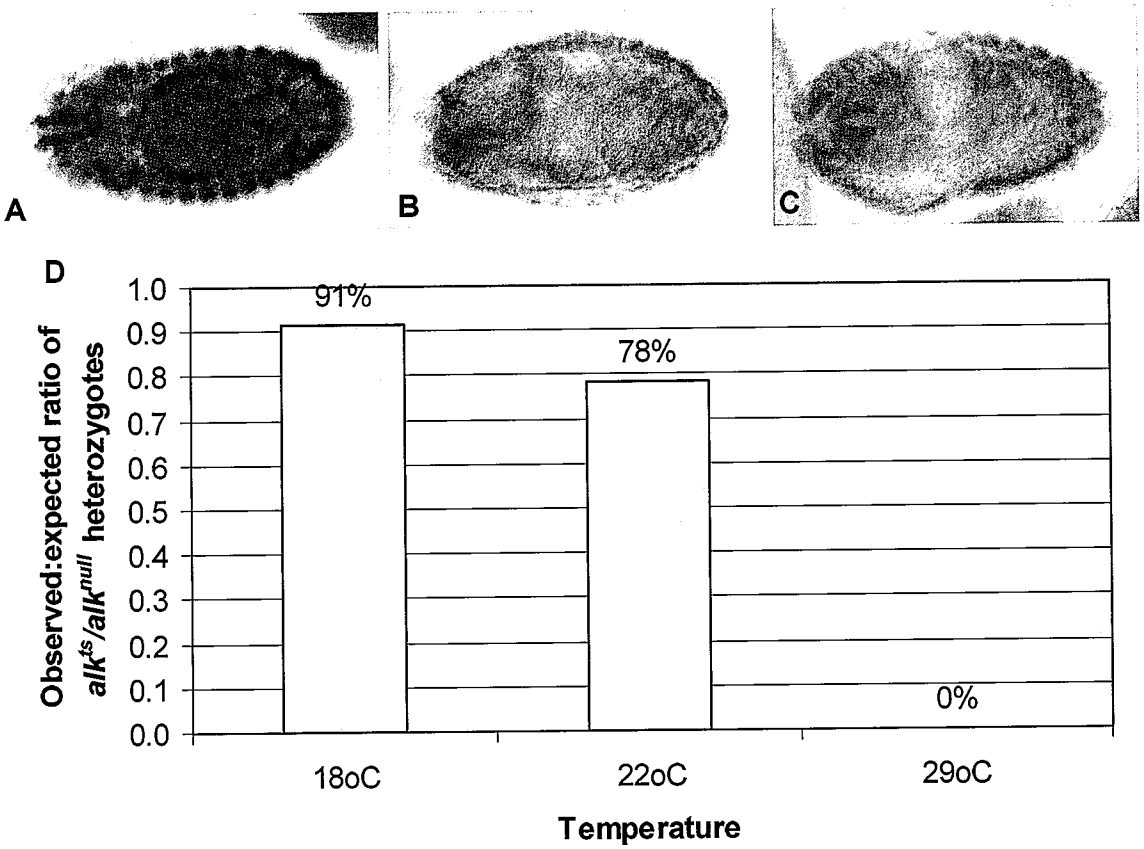

Figure 3.5. Characterization of a temperature sensitive allele of *alk*.
Dorsal views of whole mount of embryos immunostained with rabbit anti-myosin heavy chain antisera. Anterior is to the left. All embryos were collected at 29°C. (A) Control embryos heterozygous alk^{1} embryos at stage 15. Myosin heavy chain staining surrounds the midgut, and yolk is contained within the embryonic gut. Stage matched homozygous alk^{1}/alk^{1} (B) and *trans*-heterozygous $alk^{Z2\text{-}4587}/alk^{1}$ (C) embryos lack myosin staining that surrounds the gut.
(D) Observed:expected ratio of $alk^{Z2\text{-}4587}/alk^{1}$ *trans*-heterozygous adult flies at 18, 22, and 29°C. No *trans*-heterozygous $alk^{Z2\text{-}4587}/alk^{1}$ adults are obtained in the cross carried out at 29°C.

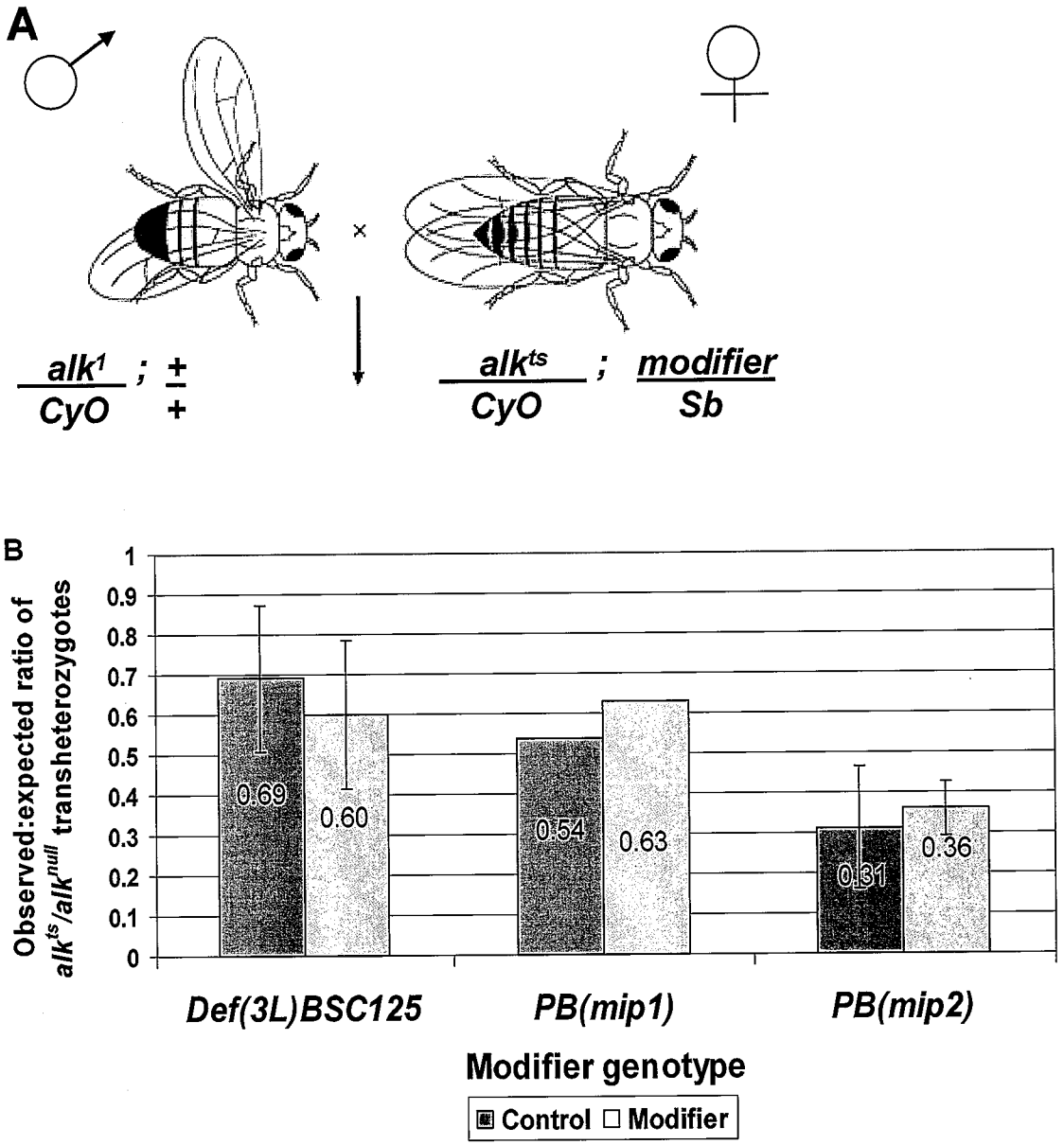

Figure 3.6. Interaction between *miple1*, *miple2*, and *alk*.
(A) Schematic for the interaction cross. *CyO* denotes marked balancer second chromosome with dominant curly wing phenotype and wild type for *alk*. *Sb* denotes marked balancer third chromosome with dominant stubble bristle phenotype and wild type for *miple1* and *miple2*.
The observed:expected ratio of $alk^{Z2\text{-}4587}/alk^{1}$ flies is calculated by dividing the total number of flies with no curly wing marker by the total number of flies with curly wings. Control flies have stubble bristles; flies in the sensitized modifier background ($miple1^{c05178}$, $miple2^{c04774}$, and *BSC125*) do not have stubble bristles.

(B) Observed:expected ratio of $alk^{Z2\text{-}4587}/alk^{1}$ *trans*-heterozygous adult flies at 23°C in the sensitized mutant (yellow) and wild type (blue) genetic backgrounds. *PB(mip1)* denotes $miple1^{c05178}$; *PB(mip2)* denotes $miple2^{c04774}$.

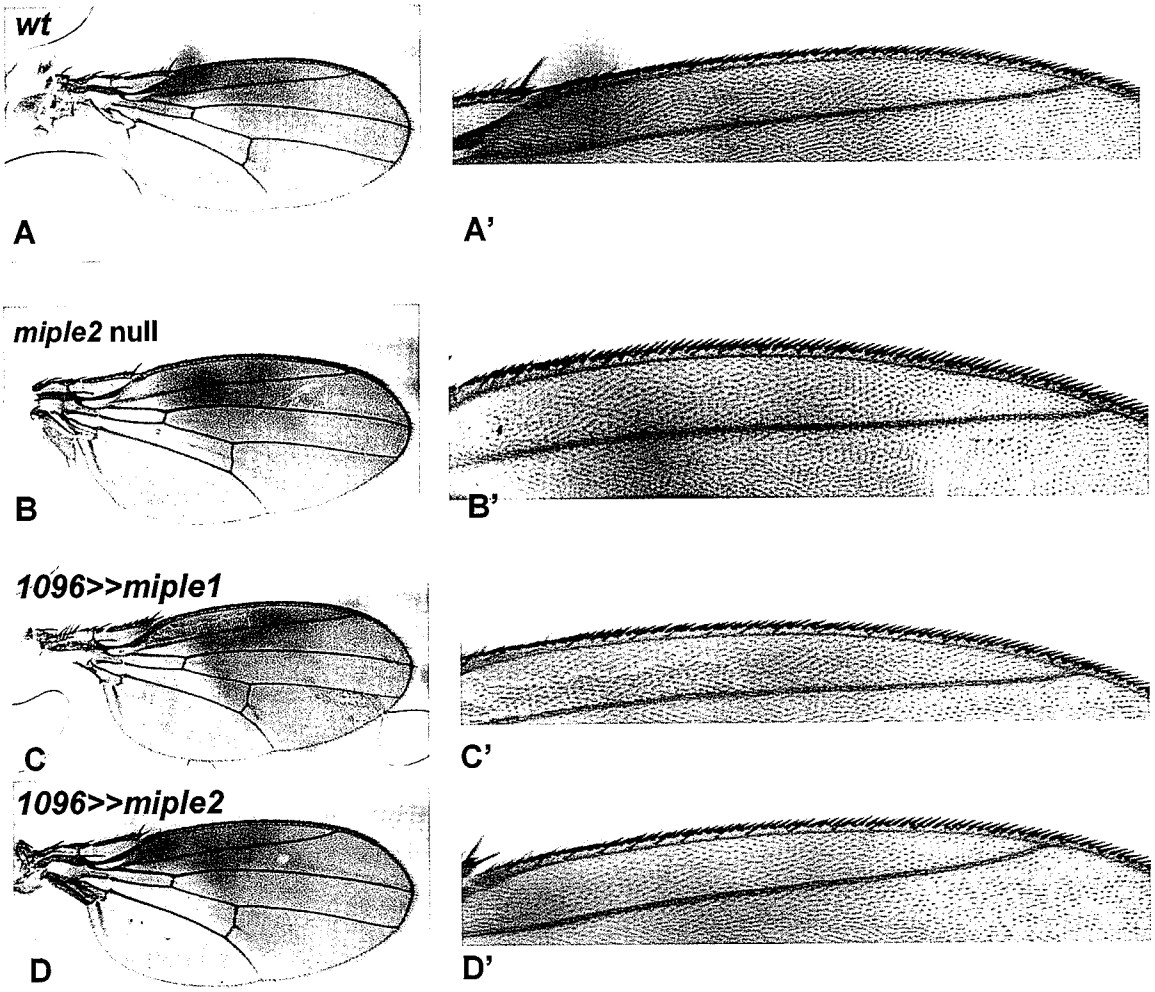

Figure 3.7. Normal adult wing patterning in *miple2*-null flies and transgenic flies overexpressing *miple1* or *miple2* in the larval imaginal disc.
Adult wings taken from wild type (A and A') and *miple2*-null *BSC125/BSC126* (B and B') flies. The *1096gal4* driver line was used to overexpress *miple1* (C and C') and *miple2* (D and D') transgenes in the larval wing disc. Vein pattern along the anteroposterior axis and bristile pattern at the wing margin are indistinguishable between all four classes of flies.

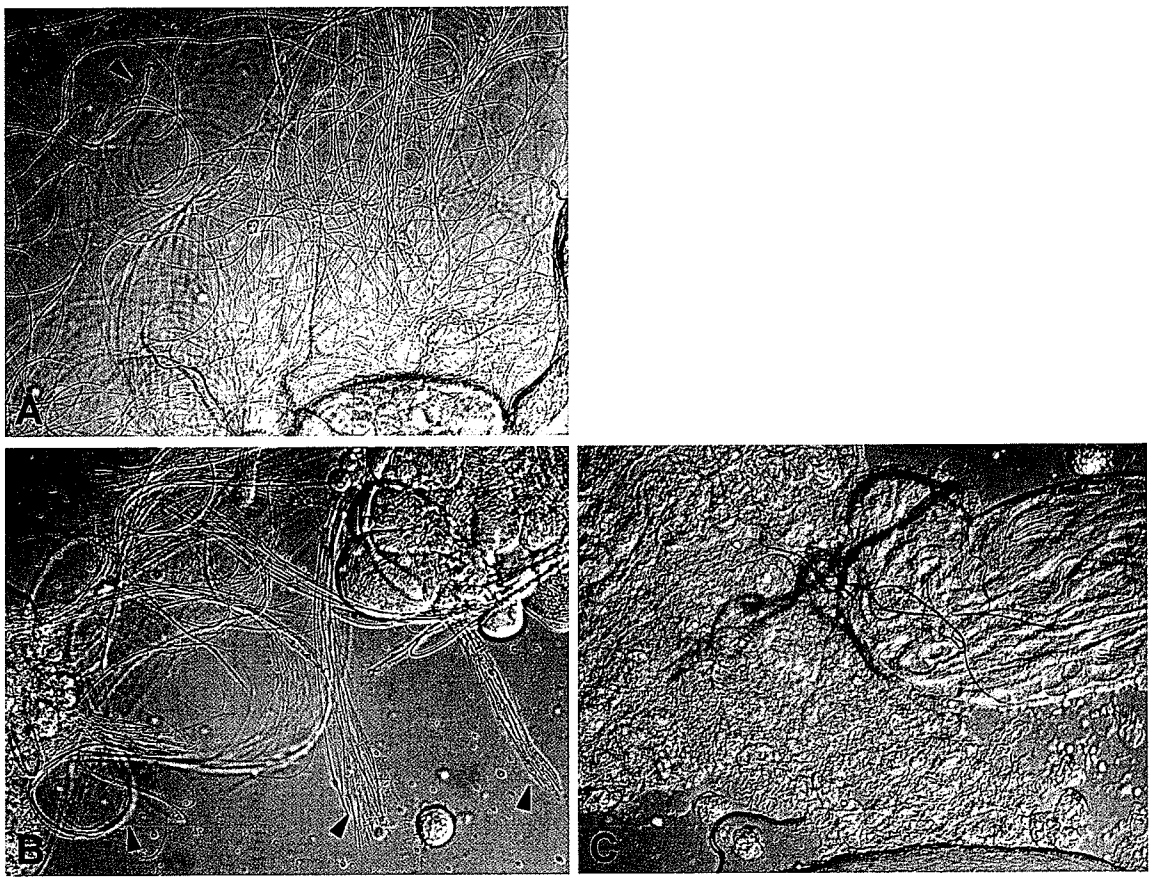
A
B
C

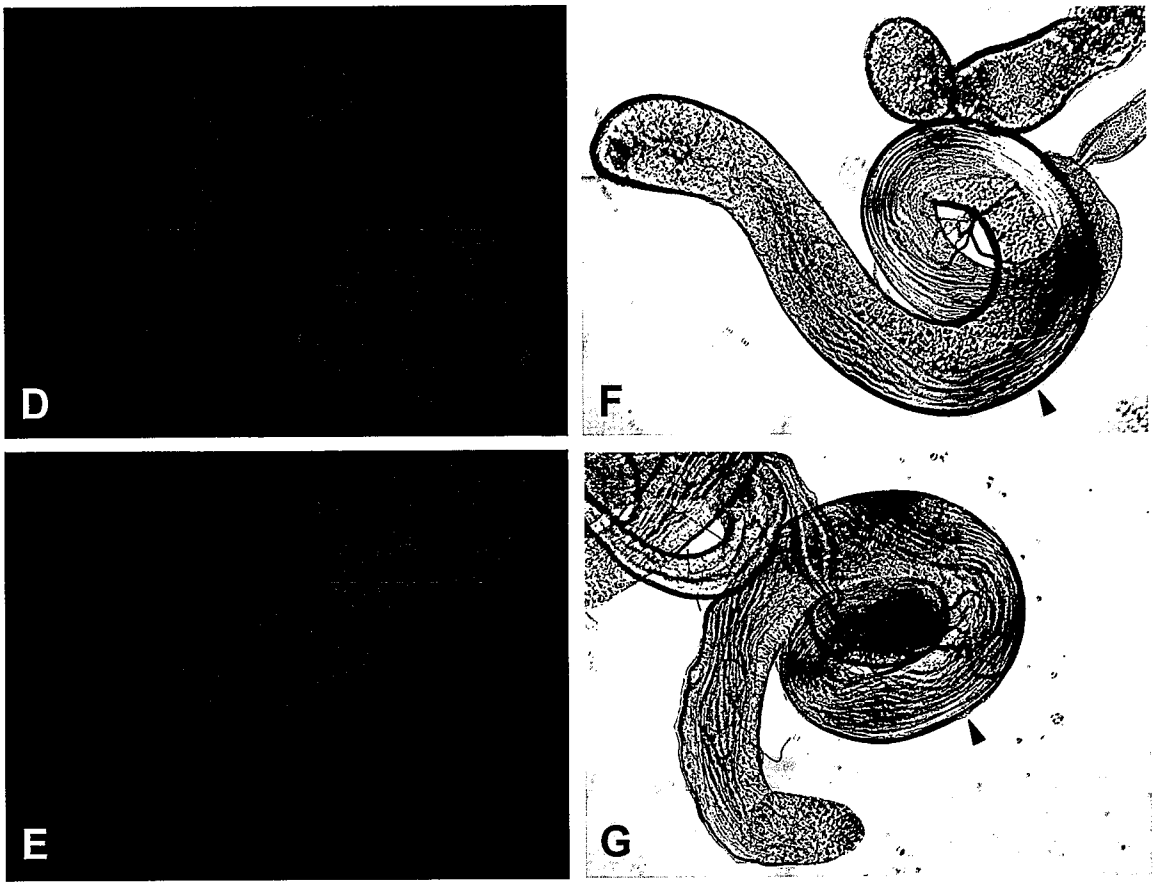

Figure 3.8. Structural analysis of *miple2*-null, *BSC125/BSC126* male reproductive system.
Phase contrast microscopy of contents released by rupturing the seminal vesicles of *BSC125* heterozygous (A) and *BSC125/BSC126* (B and C) flies. Arrowheads in (A) and (B) point to the sperm tails.
DAPI staining of testis isolated from *BSC125/BSC126* (D) and heterozygous (E) males. The patterns of staining at the apex of the testes are indistinguishable.
Phase contrast microscopy of testis squashes taken from *BSC125/BSC126* (F) and heterozygous control siblings (G). Arrowheads point to the 64-spermatid stage cysts in both images.

Thesis summary

Midkine and Pleiotrophin are secreted, heparin-binding small molecules with proposed functions in signaling. They are conserved from mamals to invertebrates. Miple1 and Miple2 are the homologues in *Drosophila*. In this study, I attempted to understand the biological functions of Midkine and Pleiotrophin by characterizing *miple1* and *miple2* during *Drosophila* development.

I presented the expression pattern of *miple1* and *miple2* in this body of work. My data suggest that *miple1* is expressed in the CNS glia during *Drosophila* embryogenesis. Embryonic *miple2* expression localizes to the endoderm and mesoderm. During larval development, *miple1* is expressed at sites within the CNS, where cells undergo proliferation. Larval expression of *miple2* is primarily localized to the imaginal discs. *miple1* mRNA localizes to the pedunculus of the adult brain, while *miple2* expression is found in the adult gonads of both males and females. My findings suggest that the expression patterns of *miple1* and *miple2* in *Drosophila* closely parallel those of Midkine and Pleiotrophin in mouse development. In addition, my work defined the specific developmental and biological processes throughout *Drosophila* life cycle for future investigations seeking to understand Midkine and Pleiotrophin function *in vivo*.

For the second half of my thesis, I used *miple2* loss-of-function mutants to investigate the requirement for *miple2* as a cofactor in Anapastic lymphoma kinase (Alk) signaling, as well signaling involving the morphogens Wingless/Wnt, Hedgehog, and Decapentaplegic/TGFβ. Using visceral mesoderm development as readout, my developmental and genetic data do not support Miple2 and Miple1 as components in Alk signaling. Phenotypic correlation using adult wing patterning does not provide conclusive

evidence that Miple2 is required as a cofactor in Wingless/Wnt, Hedgehog, and TGFβ signaling. I also reported a potential male sterile phenotype caused by defects in spermatozoa individualization in the *miple2*-null mutants.

In conclusion, my thesis work established *Drosophila* as the model organism for understanding Midkine and Pleiotrophin *in vivo*. Future investigations using the reverse genetic approach and phenotypic correlation will most likely uncover the biological roles and mechanisms underlying Midkine and Pleiotrophin function.

References

1. Kadomatsu K, Muramatsu T. Midkine and pleiotrophin in neural development and cancer. Cancer Lett 2004;204(2):127-43.
2. Kadomatsu K, Huang RP, Suganuma T, Murata F, Muramatsu T. A retinoic acid responsive gene MK found in the teratocarcinoma system is expressed in spatially and temporally controlled manner during mouse embryogenesis. The Journal of Cell Biology 1990;110(3):607-16.
3. Urios P, Duprez D, Le Caer JP, Courtois Y, Vigny M, Laurent M. Molecular cloning of RI-HB, a heparin binding protein regulated by retinoic acid. Biochemical and Biophysical Research Communications 1991;175(2):617-24.
4. Milner PG, Li YS, Hoffman RM, Kodner CM, Siegel NR, Deuel TF. A novel 17 kD heparin-binding growth factor (HBGF-8) in bovine uterus: purification and N-terminal amino acid sequence. Biochemical and Biophysical Research Communications 1989;165(3):1096-103.
5. Rauvala H. An 18-kd heparin-binding protein of developing brain that is distinct from fibroblast growth factors. The EMBO Journal 1989;8(10):2933-41.
6. Merenmies J, Rauvala H. Molecular cloning of the 18-kDa growth-associated protein of developing brain. The Journal of Biological Chemistry 1990;265(28):16721-4.
7. Tezuka K, Takeshita S, Hakeda Y, Kumegawa M, Kikuno R, Hashimoto-Gotoh T. Isolation of mouse and human cDNA clones encoding a protein expressed specifically in osteoblasts and brain tissues. Biochemical and Biophysical Research Communications 1990;173(1):246-51.

8. Courty J, Dauchel MC, Caruelle D, Perderiset M, Barritault D. Mitogenic properties of a new endothelial cell growth factor related to pleiotrophin. Biochemical and Biophysical Research Communications 1991;180(1):145-51.

9. Muramatsu H, Muramatsu T. Purification of recombinant midkine and examination of its biological activities: functional comparison of new heparin binding factors. Biochem Biophys Res Commun 1991;177(2):652-8.

10. Li YS, Milner PG, Chauhan AK, et al. Cloning and expression of a developmentally regulated protein that induces mitogenic and neurite outgrowth activity. Science (New York, NY) 1990;250(4988):1690-4.

11. Maeda N, Ichihara-Tanaka K, Kimura T, Kadomatsu K, Muramatsu T, Noda M. A receptor-like protein-tyrosine phosphatase PTPzeta/RPTPbeta binds a heparin-binding growth factor midkine. Involvement of arginine 78 of midkine in the high affinity binding to PTPzeta. J Biol Chem 1999;274(18):12474-9.

12. Maeda N, Noda M. Involvement of receptor-like protein tyrosine phosphatase zeta/RPTPbeta and its ligand pleiotrophin/heparin-binding growth-associated molecule (HB-GAM) in neuronal migration. J Cell Biol 1998;142(1):203-16.

13. Yang X, Tare RS, Partridge KA, et al. Induction of human osteoprogenitor chemotaxis, proliferation, differentiation, and bone formation by osteoblast stimulating factor-1/pleiotrophin: osteoconductive biomimetic scaffolds for tissue engineering. J Bone Miner Res 2003;18(1):47-57.

14. Qi M, Ikematsu S, Maeda N, et al. Haptotactic migration induced by midkine. Involvement of protein-tyrosine phosphatase zeta. Mitogen-activated protein

kinase, and phosphatidylinositol 3-kinase. The Journal of Biological Chemistry 2001;276(19):15868-75.

15. Takada T, Kinkori T, Muramatsu H, Hayakawa A, Torii S, Muramatsu T. Midkine, a retinoic acid-inducible heparin-binding cytokine, is a novel regulator of intracellular calcium in human neutrophils. Biochemical and Biophysical Research Communications 1997;241(3):756-61.

16. Mitsiadis TA, Salmivirta M, Muramatsu T, et al. Expression of the heparin-binding cytokines, midkine (MK) and HB-GAM (pleiotrophin) is associated with epithelial-mesenchymal interactions during fetal development and organogenesis. Development (Cambridge, England) 1995;121(1):37-51.

17. Vilar J, Lalou C, Duong VH, et al. Midkine is involved in kidney development and in its regulation by retinoids. J Am Soc Nephrol 2002;13(3):668-76.

18. Sakurai H, Bush KT, Nigam SK. Identification of pleiotrophin as a mesenchymal factor involved in ureteric bud branching morphogenesis. Development 2001;128(17):3283-93.

19. Toriyama K, Muramatsu H, Hoshino T, Torii S, Muramatsu T. Evaluation of heparin-binding growth factors in rescuing morphogenesis of heparitinase-treated mouse embryonic lung explants. Differentiation; Research in Biological Diversity 1997;61(3):161-7.

20. Owada K, Sanjo N, Kobayashi T, et al. Midkine inhibits caspase-dependent apoptosis via the activation of mitogen-activated protein kinase and phosphatidylinositol 3-kinase in cultured neurons. J Neurochem 1999;73(5):2084-92.

21. Ohuchida T, Okamoto K, Akahane K, et al. Midkine protects hepatocellular carcinoma cells against TRAIL-mediated apoptosis through down-regulation of caspase-3 activity. Cancer 2004;100(11):2430-6.

22. Tong Y, Mentlein R, Buhl R, et al. Overexpression of midkine contributes to anti-apoptotic effects in human meningiomas. Journal of Neurochemistry 2007;100(4):1097-107.

23. Takada J, Ooboshi H, Ago T, et al. Postischemic gene transfer of midkine, a neurotrophic factor, protects against focal brain ischemia. Gene Therapy 2005;12(6):487-93.

24. Qi M, Ikematsu S, Ichihara-Tanaka K, Sakuma S, Muramatsu T, Kadomatsu K. Midkine rescues Wilms' tumor cells from cisplatin-induced apoptosis: regulation of Bcl-2 expression by Midkine. Journal of Biochemistry 2000;127(2):269-77.

25. Stoica GE, Kuo A, Aigner A, et al. Identification of anaplastic lymphoma kinase as a receptor for the growth factor pleiotrophin. J Biol Chem 2001;276(20):16772-9.

26. Bowden ET, Stoica GE, Wellstein A. Anti-apoptotic signaling of pleiotrophin through its receptor, anaplastic lymphoma kinase. The Journal of Biological Chemistry 2002;277(39):35862-8.

27. Ratovitski EA, Kotzbauer PT, Milbrandt J, Lowenstein CJ, Burrow CR. Midkine induces tumor cell proliferation and binds to a high affinity signaling receptor associated with JAK tyrosine kinases. The Journal of Biological Chemistry 1998;273(6):3654-60.

28. Stoica GE, Kuo A, Powers C, et al. Midkine binds to anaplastic lymphoma kinase (ALK) and acts as a growth factor for different cell types. The Journal of Biological Chemistry 2002;277(39):35990-8.

29. Takei Y, Kadomatsu K, Matsuo S, et al. Antisense oligodeoxynucleotide targeted to Midkine, a heparin-binding growth factor, suppresses tumorigenicity of mouse rectal carcinoma cells. Cancer Research 2001;61(23):8486-91.

30. Fang W, Hartmann N, Chow DT, Riegel AT, Wellstein A. Pleiotrophin stimulates fibroblasts and endothelial and epithelial cells and is expressed in human cancer. The Journal of Biological Chemistry 1992;267(36):25889-97.

31. Souttou B, Ahmad S, Riegel AT, Wellstein A. Signal transduction pathways involved in the mitogenic activity of pleiotrophin. Implication of mitogen-activated protein kinase and phosphoinositide 3-kinase pathways. The Journal of Biological Chemistry 1997;272(31):19588-93.

32. Szabat E, Rauvala H. Role of HB-GAM (heparin-binding growth-associated molecule) in proliferation arrest in cells of the developing rat limb and its expression in the differentiating neuromuscular system. Developmental Biology 1996;178(1):77-89.

33. Hienola A, Pekkanen M, Raulo E, Vanttola P, Rauvala H. HB-GAM inhibits proliferation and enhances differentiation of neural stem cells. Molecular and Cellular Neurosciences 2004;26(1):75-88.

34. Laaroubi K, Delbe J, Vacherot F, et al. Mitogenic and in vitro angiogenic activity of human recombinant heparin affin regulatory peptide. Growth Factors (Chur, Switzerland) 1994;10(2):89-98.

35. Yeh HJ, He YY, Xu J, Hsu CY, Deuel TF. Upregulation of pleiotrophin gene expression in developing microvasculature, macrophages, and astrocytes after acute ischemic brain injury. J Neurosci 1998;18(10):3699-707.

36. Choudhuri R, Zhang HT, Donnini S, Ziche M, Bicknell R. An angiogenic role for the neurokines midkine and pleiotrophin in tumorigenesis. Cancer Res 1997;57(9):1814-9.

37. Christman KL, Fang Q, Kim AJ, et al. Pleiotrophin induces formation of functional neovasculature in vivo. Biochemical and Biophysical Research Communications 2005;332(4):1146-52.

38. Souttou B, Raulais D, Vigny M. Pleiotrophin induces angiogenesis: involvement of the phosphoinositide-3 kinase but not the nitric oxide synthase pathways. Journal of Cellular Physiology 2001;187(1):59-64.

39. Heroult M, Bernard-Pierrot I, Delbe J, et al. Heparin affin regulatory peptide binds to vascular endothelial growth factor (VEGF) and inhibits VEGF-induced angiogenesis. Oncogene 2004;23(9):1745-53.

40. Iwahara T, Fujimoto J, Wen D, et al. Molecular characterization of ALK, a receptor tyrosine kinase expressed specifically in the nervous system. Oncogene 1997;14(4):439-49.

41. Schlessinger J. Cell signaling by receptor tyrosine kinases. Cell 2000;103(2):211-25.

42. Morris SW, Kirstein MN, Valentine MB, et al. Fusion of a kinase gene, ALK, to a nucleolar protein gene, NPM, in non-Hodgkin's lymphoma. Science (New York, NY) 1994;263(5151):1281-4.

43. Morris SW, Naeve C, Mathew P, et al. ALK, the chromosome 2 gene locus altered by the t(2;5) in non-Hodgkin's lymphoma, encodes a novel neural receptor tyrosine kinase that is highly related to leukocyte tyrosine kinase (LTK). Oncogene 1997;14(18):2175-88.

44. Kuo AH, Stoica GE, Riegel AT, Wellstein A. Recruitment of insulin receptor substrate-1 and activation of NF-kappaB essential for midkine growth signaling through anaplastic lymphoma kinase. Oncogene 2007;26(6):859-69.

45. Vernersson E, Khoo NK, Henriksson ML, Roos G, Palmer RH, Hallberg B. Characterization of the expression of the ALK receptor tyrosine kinase in mice. Gene Expr Patterns 2006;6(5):448-61.

46. Maeda N, Hamanaka H, Shintani T, Nishiwaki T, Noda M. Multiple receptor-like protein tyrosine phosphatases in the form of chondroitin sulfate proteoglycan. FEBS Letters 1994;354(1):67-70.

47. Krueger NX, Saito H. A human transmembrane protein-tyrosine-phosphatase, PTP zeta, is expressed in brain and has an N-terminal receptor domain homologous to carbonic anhydrases. Proceedings of the National Academy of Sciences of the United States of America 1992;89(16):7417-21.

48. Majeti R, Bilwes AM, Noel JP, Hunter T, Weiss A. Dimerization-induced inhibition of receptor protein tyrosine phosphatase function through an inhibitory wedge. Science (New York, NY) 1998;279(5347):88-91.

49. Desai DM, Sap J, Schlessinger J, Weiss A. Ligand-mediated negative regulation of a chimeric transmembrane receptor tyrosine phosphatase. Cell 1993;73(3):541-54.

50. Bilwes AM, den Hertog J, Hunter T, Noel JP. Structural basis for inhibition of receptor protein-tyrosine phosphatase-alpha by dimerization. Nature 1996;382(6591):555-9.

51. Huber AB, Kolodkin AL, Ginty DD, Cloutier JF. Signaling at the growth cone: ligand-receptor complexes and the control of axon growth and guidance. Annual Review of Neuroscience 2003;26:509-63.

52. Maeda N, Nishiwaki T, Shintani T, Hamanaka H, Noda M. 6B4 proteoglycan/phosphacan, an extracellular variant of receptor-like protein-tyrosine phosphatase zeta/RPTPbeta, binds pleiotrophin/heparin-binding growth-associated molecule (HB-GAM). The Journal of Biological Chemistry 1996;271(35):21446-52.

53. Meng K, Rodriguez-Pena A, Dimitrov T, et al. Pleiotrophin signals increased tyrosine phosphorylation of beta beta-catenin through inactivation of the intrinsic catalytic activity of the receptor-type protein tyrosine phosphatase beta/zeta. Proceedings of the National Academy of Sciences of the United States of America 2000;97(6):2603-8.

54. Pariser H, Ezquerra L, Herradon G, Perez-Pinera P, Deuel TF. Fyn is a downstream target of the pleiotrophin/receptor protein tyrosine phosphatase beta/zeta-signaling pathway: regulation of tyrosine phosphorylation of Fyn by pleiotrophin. Biochemical and Biophysical Research Communications 2005;332(3):664-9.

55. Pariser H, Perez-Pinera P, Ezquerra L, Herradon G, Deuel TF. Pleiotrophin stimulates tyrosine phosphorylation of beta-adducin through inactivation of the

transmembrane receptor protein tyrosine phosphatase beta/zeta. Biochemical and Biophysical Research Communications 2005;335(1):232-9.

56. Sakaguchi N, Muramatsu H, Ichihara-Tanaka K, et al. Receptor-type protein tyrosine phosphatase zeta as a component of the signaling receptor complex for midkine-dependent survival of embryonic neurons. Neuroscience Research 2003;45(2):219-24.

57. Levy JB, Canoll PD, Silvennoinen O, et al. The cloning of a receptor-type protein tyrosine phosphatase expressed in the central nervous system. The Journal of Biological Chemistry 1993;268(14):10573-81.

58. Tamura H, Fukada M, Fujikawa A, Noda M. Protein tyrosine phosphatase receptor type Z is involved in hippocampus-dependent memory formation through dephosphorylation at Y1105 on p190 RhoGAP. Neuroscience Letters 2006;399(1-2):33-8.

59. Nakamura E, Kadomatsu K, Yuasa S, et al. Disruption of the midkine gene (Mdk) resulted in altered expression of a calcium binding protein in the hippocampus of infant mice and their abnormal behaviour. Genes Cells 1998;3(12):811-22.

60. Pavlov I, Voikar V, Kaksonen M, et al. Role of heparin-binding growth-associated molecule (HB-GAM) in hippocampal LTP and spatial learning revealed by studies on overexpressing and knockout mice. Molecular and Cellular Neurosciences 2002;20(2):330-42.

61. Nakanishi T, Kadomatsu K, Okamoto T, et al. Expression of syndecan-1 and -3 during embryogenesis of the central nervous system in relation to binding with midkine. Journal of Biochemistry 1997;121(2):197-205.

62. Kojima T, Katsumi A, Yamazaki T, et al. Human ryudocan from endothelium-like cells binds basic fibroblast growth factor, midkine, and tissue factor pathway inhibitor. The Journal of Biological Chemistry 1996;271(10):5914-20.

63. Raulo E, Chernousov MA, Carey DJ, Nolo R, Rauvala H. Isolation of a neuronal cell surface receptor of heparin binding growth-associated molecule (HB-GAM). Identification as N-syndecan (syndecan-3). The Journal of Biological Chemistry 1994;269(17):12999-3004.

64. Kurosawa N, Chen GY, Kadomatsu K, Ikematsu S, Sakuma S, Muramatsu T. Glypican-2 binds to midkine: the role of glypican-2 in neuronal cell adhesion and neurite outgrowth. Glycoconjugate Journal 2001;18(6):499-507.

65. Ichihara-Tanaka K, Oohira A, Rumsby M, Muramatsu T. Neuroglycan C is a novel midkine receptor involved in process elongation of oligodendroglial precursor-like cells. The Journal of Biological Chemistry 2006;281(41):30857-64.

66. Zou K, Muramatsu H, Ikematsu S, et al. A heparin-binding growth factor, midkine, binds to a chondroitin sulfate proteoglycan, PG-M/versican. European Journal of Biochemistry / FEBS 2000;267(13):4046-53.

67. Muramatsu H, Zou K, Sakaguchi N, Ikematsu S, Sakuma S, Muramatsu T. LDL receptor-related protein as a component of the midkine receptor. Biochemical and Biophysical Research Communications 2000;270(3):936-41.

68. Shibata Y, Muramatsu T, Hirai M, et al. Nuclear targeting by the growth factor midkine. Molecular and Cellular Biology 2002;22(19):6788-96.

69. Iwasaki W, Nagata K, Hatanaka H, et al. Solution structure of midkine, a new heparin-binding growth factor. The EMBO Journal 1997;16(23):6936-46.

70. Kilpelainen I, Kaksonen M, Kinnunen T, et al. Heparin-binding growth-associated molecule contains two heparin-binding beta -sheet domains that are homologous to the thrombospondin type I repeat. The Journal of Biological Chemistry 2000;275(18):13564-70.

71. Bork P. The modular architecture of a new family of growth regulators related to connective tissue growth factor. FEBS Letters 1993;327(2):125-30.

72. Fabri L, Maruta H, Muramatsu H, et al. Structural characterisation of native and recombinant forms of the neurotrophic cytokine MK. Journal of Chromatography 1993;646(1):213-25.

73. Fabri L, Nice EC, Ward LD, Maruta H, Burgess AW, Simpson RJ. Characterization of bovine heparin-binding neurotrophic factor (HBNF): assignment of disulfide bonds. Biochemistry International 1992;28(1):1-9.

74. Muramatsu H, Inui T, Kimura T, et al. Localization of heparin-binding, neurite outgrowth and antigenic regions in midkine molecule. Biochemical and Biophysical Research Communications 1994;203(2):1131-9.

75. Inui T, Nakao M, Nishio H, et al. Solution synthesis and biological activity of human pleiotrophin, a novel heparin-binding neurotrophic factor consisting of 136 amino acid residues with five disulfide bonds. J Pept Res 2000;55(5):384-97.

76. Asai T, Watanabe K, Ichihara-Tanaka K, et al. Identification of heparin-binding sites in midkine and their role in neurite-promotion. Biochemical and Biophysical Research Communications 1997;236(1):66-70.

77. Zhang N, Zhong R, Deuel TF. Domain structure of pleiotrophin required for transformation. The Journal of Biological Chemistry 1999;274(19):12959-62.

78. Raulo E, Tumova S, Pavlov I, et al. The two thrombospondin type I repeat domains of the heparin-binding growth-associated molecule bind to heparin/heparan sulfate and regulate neurite extension and plasticity in hippocampal neurons. The Journal of Biological Chemistry 2005;280(50):41576-83.

79. Silos-Santiago I, Yeh HJ, Gurrieri MA, et al. Localization of pleiotrophin and its mRNA in subpopulations of neurons and their corresponding axonal tracts suggests important roles in neural-glial interactions during development and in maturity. J Neurobiol 1996;31(3):283-96.

80. Fan QW, Muramatsu T, Kadomatsu K. Distinct expression of midkine and pleiotrophin in the spinal cord and placental tissues during early mouse development. Dev Growth Differ 2000;42(2):113-9.

81. Amet LE, Lauri SE, Hienola A, et al. Enhanced hippocampal long-term potentiation in mice lacking heparin-binding growth-associated molecule. Mol Cell Neurosci 2001;17(6):1014-24.

82. Matsumoto K, Wanaka A, Mori T, et al. Localization of pleiotrophin and midkine in the postnatal developing cerebellum. Neuroscience Letters 1994;178(2):216-20.

83. Reynolds PR, Mucenski ML, Whitsett JA. Thyroid transcription factor (TTF) -1 regulates the expression of midkine (MK) during lung morphogenesis. Dev Dyn 2003;227(2):227-37.

84. Wisniewski T, Lalowski M, Baumann M, et al. HB-GAM is a cytokine present in Alzheimer's and Down's syndrome lesions. Neuroreport 1996;7(2):667-71.

85. Yasuhara O, Muramatsu H, Kim SU, Muramatsu T, Maruta H, McGeer PL. Midkine, a novel neurotrophic factor, is present in senile plaques of Alzheimer disease. Biochemical and Biophysical Research Communications 1993;192(1):246-51.

86. Salama RH, Muramatsu H, Shimizu E, et al. Increased midkine levels in sera from patients with Alzheimer's disease. Progress in Neuro-psychopharmacology & Biological Psychiatry 2005;29(4):611-6.

87. Yasuhara O, Schwab C, Matsuo A, et al. Midkine-like immunoreactivity in extracellular neurofibrillary tangles in brains of patients with parkinsonism-dementia complex of Guam. Neuroscience Letters 1996;205(2):107-10.

88. Pufe T, Bartscher M, Petersen W, Tillmann B, Mentlein R. Expression of pleiotrophin, an embryonic growth and differentiation factor, in rheumatoid arthritis. Arthritis and Rheumatism 2003;48(3):660-7.

89. Takada T, Toriyama K, Muramatsu H, Song XJ, Torii S, Muramatsu T. Midkine, a retinoic acid-inducible heparin-binding cytokine in inflammatory responses: chemotactic activity to neutrophils and association with inflammatory synovitis. Journal of Biochemistry 1997;122(2):453-8.

90. Maekawa T, Waki S, Okada A, Fukui H, Kinoshita Y, Chiba T. Midkine gene expression in the healing process of gastric ulcer. The Journal of Laboratory and Clinical Medicine 1999;133(4):349-52.

91. Yuki T, Ishihara S, Rumi MA, et al. Increased expression of midkine in the rat colon during healing of experimental colitis. American Journal of Physiology 2006;291(4):G735-43.

92. Florin L, Maas-Szabowski N, Werner S, Szabowski A, Angel P. Increased keratinocyte proliferation by JUN-dependent expression of PTN and SDF-1 in fibroblasts. Journal of Cell Science 2005;118(Pt 9):1981-9.

93. Yoshida Y, Goto M, Tsutsui J, et al. Midkine is present in the early stage of cerebral infarct. Brain Research 1995;85(1):25-30.

94. Wada M, Kamata M, Aizu Y, Morita T, Hu J, Oyanagi K. Alteration of midkine expression in the ischemic brain of humans. Journal of the Neurological Sciences 2002;200(1-2):67-73.

95. Obama H, Biro S, Tashiro T, et al. Myocardial infarction induces expression of midkine, a heparin-binding growth factor with reparative activity. Anticancer Research 1998;18(1A):145-52.

96. Horiba M, Kadomatsu K, Yasui K, et al. Midkine plays a protective role against cardiac ischemia/reperfusion injury through a reduction of apoptotic reaction. Circulation 2006;114(16):1713-20.

97. Herradon G, Ezquerra L, Nguyen T, Silos-Santiago I, Deuel TF. Midkine regulates pleiotrophin organ-specific gene expression: evidence for transcriptional regulation and functional redundancy within the pleiotrophin/midkine developmental gene family. Biochemical and Biophysical Research Communications 2005;333(3):714-21.

98. Zou P, Muramatsu H, Sone M, Hayashi H, Nakashima T, Muramatsu T. Mice doubly deficient in the midkine and pleiotrophin genes exhibit deficits in the expression of beta-tectorin gene and in auditory response. Laboratory Investigation; a Journal of Technical Methods and Pathology 2006;86(7):645-53.

99. Muramatsu H, Zou P, Kurosawa N, et al. Female infertility in mice deficient in midkine and pleiotrophin, which form a distinct family of growth factors. Genes Cells 2006;11(12):1405-17.

100. Englund C, Birve A, Falileeva L, Grabbe C, Palmer RH. Miple1 and miple2 encode a family of MK/PTN homologues in *Drosophila* melanogaster. Development Genes and Evolution 2006;216(1):10-8.

101. Muramatsu T. Midkine and pleiotrophin: two related proteins involved in development, survival, inflammation and tumorigenesis. J Biochem (Tokyo) 2002;132(3):359-71.

102. St Johnston D. The art and design of genetic screens: *Drosophila* melanogaster. Nat Rev Genet 2002;3(3):176-88.

103. Winkler S, Schwabedissen A, Backasch D, et al. Target-selected mutant screen by TILLING in *Drosophila*. Genome Res 2005;15(5):718-23.

104. Parks AL, Cook KR, Belvin M, et al. Systematic generation of high-resolution deletion coverage of the *Drosophila* melanogaster genome. Nat Genet 2004;36(3):288-92.

105. Thibault ST, Singer MA, Miyazaki WY, et al. A complementary transposon tool kit for *Drosophila* melanogaster using P and piggyBac. Nat Genet 2004;36(3):283-7.

106. Jacobs JR, Goodman CS. Embryonic development of axon pathways in the *Drosophila* CNS. I. A glial scaffold appears before the first growth cones. J Neurosci 1989;9(7):2402-11.

107. Klambt C, Jacobs JR, Goodman CS. The midline of the *Drosophila* central nervous system: a model for the genetic analysis of cell fate, cell migration, and growth cone guidance. Cell 1991;64(4):801-15.

108. Zhang N, Yeh HJ, Zhong R, Li YS, Deuel TF. A dominant-negative pleiotrophin mutant introduced by homologous recombination leads to germ-cell apoptosis in male mice. Proc Natl Acad Sci U S A 1999;96(12):6734-8.

109. Spring J, Paine-Saunders SE, Hynes RO, Bernfield M. *Drosophila* syndecan: conservation of a cell-surface heparan sulfate proteoglycan. Proc Natl Acad Sci U S A 1994;91(8):3334-8.

110. Nakato H, Futch TA, Selleck SB. The division abnormally delayed (dally) gene: a putative integral membrane proteoglycan required for cell division patterning during postembryonic development of the nervous system in *Drosophila*. Development 1995;121(11):3687-702.

111. Khare N, Baumgartner S. Dally-like protein, a new *Drosophila* glypican with expression overlapping with wingless. Mech Dev 2000;99(1-2):199-202.

112. Lin X, Perrimon N. Dally cooperates with *Drosophila* Frizzled 2 to transduce Wingless signalling. Nature 1999;400(6741):281-4.

113. Kirkpatrick CA, Dimitroff BD, Rawson JM, Selleck SB. Spatial regulation of Wingless morphogen distribution and signaling by Dally-like protein. Dev Cell 2004;7(4):513-23.

114. Kreuger J, Perez L, Giraldez AJ, Cohen SM. Opposing activities of Dally-like glypican at high and low levels of Wingless morphogen activity. Dev Cell 2004;7(4):503-12.

115. Han C, Belenkaya TY, Wang B, Lin X. *Drosophila* glypicans control the cell-to-cell movement of Hedgehog by a dynamin-independent process. Development 2004;131(3):601-11.

116. Jackson SM, Nakato H, Sugiura M, et al. dally, a *Drosophila* glypican, controls cellular responses to the TGF-beta-related morphogen, Dpp. Development 1997;124(20):4113-20.

117. Yan D, Lin X. *Drosophila* glypican Dally-like acts in FGF-receiving cells to modulate FGF signaling during tracheal morphogenesis. Dev Biol 2007.

118. Desbordes SC, Sanson B. The glypican Dally-like is required for Hedgehog signalling in the embryonic epidermis of *Drosophila*. Development 2003;130(25):6245-55.

119. Hariharan IK, Chuang PT, Rubin GM. Cloning and characterization of a receptor-class phosphotyrosine phosphatase gene expressed on central nervous system axons in *Drosophila* melanogaster. Proceedings of the National Academy of Sciences of the United States of America 1991;88(24):11266-70.

120. Oon SH, Hong A, Yang X, Chia W. Alternative splicing in a novel tyrosine phosphatase gene (DPTP4E) of *Drosophila* melanogaster generates two large receptor-like proteins which differ in their carboxyl termini. The Journal of Biological Chemistry 1993;268(32):23964-71.

121. Tian SS, Tsoulfas P, Zinn K. Three receptor-linked protein-tyrosine phosphatases are selectively expressed on central nervous system axons in the *Drosophila* embryo. Cell 1991;67(4):675-85.

122. Yang XH, Seow KT, Bahri SM, Oon SH, Chia W. Two *Drosophila* receptor-like tyrosine phosphatase genes are expressed in a subset of developing axons and pioneer neurons in the embryonic CNS. Cell 1991;67(4):661-73.

123. Streuli M, Krueger NX, Tsai AY, Saito H. A family of receptor-linked protein tyrosine phosphatases in humans and *Drosophila*. Proceedings of the National Academy of Sciences of the United States of America 1989;86(22):8698-702.

124. Schindelholz B, Knirr M, Warrior R, Zinn K. Regulation of CNS and motor axon guidance in *Drosophila* by the receptor tyrosine phosphatase DPTP52F. Development (Cambridge, England) 2001;128(21):4371-82.

125. Johnson KG, Tenney AP, Ghose A, et al. The HSPGs Syndecan and Dallylike bind the receptor phosphatase LAR and exert distinct effects on synaptic development. Neuron 2006;49(4):517-31.

126. Fox AN, Zinn K. The heparan sulfate proteoglycan syndecan is an in vivo ligand for the *Drosophila* LAR receptor tyrosine phosphatase. Curr Biol 2005;15(19):1701-11.

127. Toledano-Katchalski H, Nir R, Volohonsky G, Volk T. Post-transcriptional repression of the *Drosophila* midkine and pleiotrophin homolog miple by HOW is essential for correct mesoderm spreading. Development (Cambridge, England) 2007;134(19):3473-81.

128. Loren CE, Scully A, Grabbe C, et al. Identification and characterization of DAlk: a novel *Drosophila* melanogaster RTK which drives ERK activation in vivo. Genes Cells 2001;6(6):531-44.

129. Englund C, Loren CE, Grabbe C, et al. Jeb signals through the Alk receptor tyrosine kinase to drive visceral muscle fusion. Nature 2003;425(6957):512-6.

130. Lee HH, Norris A, Weiss JB, Frasch M. Jelly belly protein activates the receptor tyrosine kinase Alk to specify visceral muscle pioneers. Nature 2003;425(6957):507-12.

131. Loren CE, Englund C, Grabbe C, Hallberg B, Hunter T, Palmer RH. A crucial role for the Anaplastic lymphoma kinase receptor tyrosine kinase in gut development in *Drosophila* melanogaster. EMBO Rep 2003;4(8):781-6.

132. Weiss JB, Suyama KL, Lee HH, Scott MP. Jelly belly: a *Drosophila* LDL receptor repeat-containing signal required for mesoderm migration and differentiation. Cell 2001;107(3):387-98.

133. Tabata T, Kornberg TB. Hedgehog is a signaling protein with a key role in patterning *Drosophila* imaginal discs. Cell 1994;76(1):89-102.

134. Couso JP, Bishop SA, Martinez Arias A. The wingless signalling pathway and the patterning of the wing margin in *Drosophila*. Development 1994;120(3):621-36.

135. Zecca M, Basler K, Struhl G. Sequential organizing activities of engrailed, hedgehog and decapentaplegic in the *Drosophila* wing. Development 1995;121(8):2265-78.

136. Azpiazu N, Lawrence PA, Vincent JP, Frasch M. Segmentation and specification of the *Drosophila* mesoderm. Genes Dev 1996;10(24):3183-94.

137. Fuller MT. Genetic control of cell proliferation and differentiation in *Drosophila* spermatogenesis. Semin Cell Dev Biol 1998;9(4):433-44.

138. Schulz C, Wood CG, Jones DL, Tazuke SI, Fuller MT. Signaling from germ cells mediated by the rhomboid homolog stet organizes encapsulation by somatic support cells. Development 2002;129(19):4523-34.

139. Matunis E, Tran J, Gonczy P, Caldwell K, DiNardo S. punt and schnurri regulate a somatically derived signal that restricts proliferation of committed progenitors in the germline. Development 1997;124(21):4383-91.

140. Kawase E, Wong MD, Ding BC, Xie T. Gbb/Bmp signaling is essential for maintaining germline stem cells and for repressing bam transcription in the *Drosophila* testis. Development 2004;131(6):1365-75.

141. Brand AH, Perrimon N. Targeted gene expression as a means of altering cell fates and generating dominant phenotypes. Development 1993;118(2):401-15.

142. Hicks MS, O'Leary V, Wilkin M, Bee SE, Humphries MJ, Baron M. DrhoGEF3 encodes a new *Drosophila* DH domain protein that exhibits a highly dynamic embryonic expression pattern. Development Genes and Evolution 2001;211(5):263-7.

143. Wakimoto BT, Lindsley DL, Herrera C. Toward a comprehensive genetic analysis of male fertility in *Drosophila* melanogaster. Genetics 2004;167(1):207-16.

144. Perez-Pinera P, Zhang W, Chang Y, Vega JA, Deuel TF. Anaplastic lymphoma kinase is activated through the pleiotrophin/receptor protein-tyrosine phosphatase beta/zeta signaling pathway: an alternative mechanism of receptor tyrosine kinase activation. J Biol Chem 2007;282(39):28683-90.

145. Mathivet T, Mazot P, Vigny M. In contrast to agonist monoclonal antibodies, both C-terminal truncated form and full length form of Pleiotrophin failed to activate vertebrate ALK (anaplastic lymphoma kinase)? Cell Signal 2007;19(12):2434-43.

146. Fabrizio JJ, Hime G, Lemmon SK, Bazinet C. Genetic dissection of sperm individualization in *Drosophila* melanogaster. Development 1998;125(10):1833-43.